

การแจกแจงผลิตภัณฑ์จากการแตกตัวด้วยไฮโดรเจนของโคพอลิเมอร์สไตรีน
อะครีโลไนไทรล์ บน HZSM-5



นางรัตนา บุญประเสริฐ

สถาบันวิทยบริการ
จุฬาลงกรณ์มหาวิทยาลัย

วิทยานิพนธ์นี้เป็นส่วนหนึ่งของการศึกษาตามหลักสูตรปริญญาวิทยาศาสตรมหาบัณฑิต

สาขาวิชาปิโตรเคมีและวิทยาศาสตร์พอลิเมอร์

คณะวิทยาศาสตร์ จุฬาลงกรณ์มหาวิทยาลัย

ปีการศึกษา 2546

ISBN 974-17-4548-6

ลิขสิทธิ์ของจุฬาลงกรณ์มหาวิทยาลัย

PRODUCT DISTRIBUTION FROM HYDROCRACKING OF STYRENE-
ACRYLONITRILE COPOLYMER ON HZSM-5



Mrs.Rattana Boonprasert

สถาบันวิทยบริการ
จุฬาลงกรณ์มหาวิทยาลัย

A Thesis Submitted in Partial Fulfillment of the Requirements

for the Degree of Master of Science in Petrochemistry and Polymer Science

Faculty of Science

Chulalongkorn University

Academic Year 2003

ISBN 974-17-4548-6

Thesis Title PRODUCT DISTRIBUTION FROM HYDROCRACKING OF
 STYRENE-ACRYLONITRILE COPOLYMER ON HZSM-5

By Mrs.Rattana Boonprasert

Field of study Petrochemistry and Polymer Science

Thesis Advisor Associate Professor Tharapong Vitidsant, Ph.D.

Accepted by the Faculty of Science, Chulalongkorn University in Partial
Fulfillment of the Requirements for the Master's Degree

.....Dean of Faculty of Science
(Professor Piamsak Menasveta, Ph.D.)

THESIS COMMITTEE

.....Chairman
(Professor Pattarapan Prasassarakich, Ph.D.)

.....Thesis Advisor
(Associate Professor Tharapong Vitidsant, Ph.D.)

.....Member
(Assistant Professor Warinthorn Chavasiri, Ph.D.)

.....Member
(Suchaya Nitivattananon, Ph.D.)

รัตนา บุญประเสริฐ : การแจกแจงผลิตภัณฑ์จากการแตกตัวด้วยไฮโดรเจนของ
โคพอลิเมอร์สไตรีน-อะครีโลไนไทรล์บน HZSM-5 (PRODUCT
DISTRIBUTION FROM HYDROCRACKING OF STYRENE-
ACRYLONITRILE COPOLYMER ON HZSM-5) อ.ที่ปรึกษา : รศ.ดร.ธราพงษ์
วิทิตสานต์, จำนวน 99 หน้า ISBN 974-17-4548-6.

จุดมุ่งหมายหลักของงานวิจัยนี้ มุ่งที่จะศึกษาการกระจายตัวของผลิตภัณฑ์น้ำมัน
ที่ได้จากการแตกตัวโคพอลิเมอร์สไตรีนอะครีโลไนไทรล์ บนตัวเร่งปฏิกิริยา HZSM-5
ในเครื่องปฏิกรณ์ขนาดเล็ก ซึ่งมีเส้นผ่านศูนย์กลางภายใน 30 มิลลิเมตรและปริมาตร 70
มิลลิลิตร โดยการเปลี่ยนแปลงค่าตัวแปรดังนี้ อุณหภูมิของปฏิกิริยาระหว่าง 380-450
องศาเซลเซียส ปริมาณตัวเร่งปฏิกิริยาระหว่าง 0-2.5% โดยน้ำหนัก เวลาที่ใช้ในการทำ
ปฏิกิริยาระหว่าง 30-90 นาที และความดันของก๊าซไฮโดรเจนระหว่าง 0-300 psig

ผลิตภัณฑ์น้ำมันที่วิเคราะห์โดยใช้เครื่องก๊าซโครมาโตกราฟีชนิดจำลองการ
กลั่น พบว่า HZSM-5 เป็นตัวเร่งปฏิกิริยาที่เหมาะสม ในการแตกโคพอลิเมอร์สไตรีน
อะครีโลไนไทรล์ โดยภาวะที่เหมาะสมในการทำปฏิกิริยามีดังต่อไปนี้ อุณหภูมิ 430
องศาเซลเซียส ปริมาณตัวเร่งปฏิกิริยา 1.25% โดยน้ำหนัก เวลาในการทำปฏิกิริยา 60
นาที และความดันของก๊าซไฮโดรเจน 200 psig ผลิตภัณฑ์น้ำมันที่ได้มีปริมาณเนฟทา
45.07%, เคโรซีน 6.03%, ก๊าซออยล์ 12.41% และโมเลกุลสายยาว 11.95% นอกจากนี้
จากอินฟราเรดสเปกตรัม พบหมู่ฟังก์ชันของสารประกอบอะโรมาติก เช่นเดียวกับ
สเปกตรัมของน้ำมันเบนซิน 95

สาขาวิชา ปิโตรเคมีและวิทยาศาสตร์พอลิเมอร์ ลายมือชื่อนักศึกษา.....
ปีการศึกษา 2546 ลายมือชื่ออาจารย์ที่ปรึกษา.....

4573411923 : MAJOR PETROCHEMISTRY AND POLYMER SCIENCE

KEY WORD: CONVERSION / SAN / HZSM-5 / CATALYTIC CRACKING

RATTANA BOONPRASERT: PRODUCT DISTRIBUTION FROM HYDROCRACKING OF STYRENE-ACRYLONITRILE COPOLYMER ON HZSM-5. THESIS ADVISOR: ASSOCIATE PROFESSOR THARAPONG VITIDSANT, Ph.D.,

The main objective of this research was aimed to study the distribution of oil product from cracking styrene-acrylonitrile copolymer using HZSM-5 catalyst. Experiment was done in a microreactor width of 30 mm inside diameter and volume of 70 ml by varying operating conditions. Temperature and amount of catalyst were first varied between 380 to 450 °C, 0 to 2.5% by weight, respectively. While reaction time and pressure of hydrogen gas were varied between 30 to 90 min, 0 to 300 psig, respectively.

The analyzed oil product from gas chromatography (GC Simulated Distillation) was found that HZSM-5 catalyst was suitable to crack SAN. The optimum condition was 430 °C, amounts of catalyst 1.25% by weight, reaction time 60 min and hydrogen pressure at 200 psig. The product yield at this condition was in the range of 45.07% naphtha, 6.03% kerosene, 12.41% gas oil and 11.95% long residues. Moreover, the product showed aromatic functional group by means of Fourier Transform Infrared Spectrometer, same spectrum of benzene oil octane number 95.

Field of study Petrochemistry and polymer science Student's signature.....

Academic year 2003

Advisor's signature.....

ACKNOWLEDGEMENTS

The author would like to express her sincere gratitude to Associate Professor Dr. Tharapong Vitidsant for providing valuable advice and unceasing assistance towards the completion of the thesis. In addition, the author also wants to thank the thesis committees: Professor Dr.Pattarapan Prasassarakich, Assistant Professor Dr. Warinthorn Chavasiri and Dr. Suchaya Nitivattananon as chairman and members of the thesis committee, respectively, whose comments are especially helpful.

Further the author would like to thank Flg. Lt. Atsadayut Kaewsaiyoy, Mr.Apichart Charansiripaisarn and Mr.Somnuk Boonprasert for their assistance. Thanks are also due to everyone who has contributed suggestions and give him support for this thesis.

Finally, the author expresses her sincere thanks to her parents, her brothers and sister, for their sincere love and concern.

สถาบันวิทยบริการ
จุฬาลงกรณ์มหาวิทยาลัย

CONTENTS

	PAGE
ABSTRACT (IN THAI).....	iv
ABSTRACT (IN ENGLISH).....	v
ACKNOWLEDGEMENTS.....	vi
CONTENTS.....	vii
LIST OF FIGURES.....	x
LIST OF TABLES.....	xiii
CHAPTER	
I. INTRODUCTION.....	1
II. LITERATURE REVIEWS.....	4
Styrene Acrylonitrile Copolymer (SAN).....	4
2.1 The production of SAN Copolymer.....	4
2.1.1 Emulsion polymerization process.....	5
2.1.2 Suspension polymerization process.....	5
2.1.3 Bulk polymerization process.....	5
2.2 Physical and chemical properties.....	6
2.3 Processing and application.....	8
2.4 Literature Reviews.....	9
III. THEORY.....	14
3.1 Introduction.....	14
3.2 History of Zeolites.....	16
3.2.1 Previous history.....	16
3.2.2 Industrial history.....	17
3.2.2.1 Synthetic zeolites.....	17
3.2.2.2 Natural zeolites.....	18

CONTENTS (Continued)

CHAPTER	Page
3.3 Structure of Zeolite.....	19
3.3.1 Pore size.....	23
3.3.1.1 Small pore zeolites.....	23
3.3.1.2 Medium pore zeolites.....	24
3.3.1.3 Large pore zeolites.....	25
3.4 X and Y zeolite structures.....	26
3.5 Zeolites as Catalysts.....	28
3.5.1 Potential versatility of zeolites as catalysts.....	28
3.5.1.1 Crystal voidage and channels.....	28
3.5.1.2 Variable pore sizes.....	30
3.5.1.3 Ion exchange.....	30
3.5.1.4 Salt occlusion.....	31
3.5.1.5 Framework modification.....	31
3.6 Zeolite Active sites.....	32
3.6.1 Acid sites.....	32
3.6.2 Generation of acid centers.....	33
3.6.3 Basic sites.....	37
3.7 Shape-selectivity Catalysis.....	38
3.8 Mechanism of Cracking Processes.....	43
3.8.1 Thermal cracking.....	43
3.8.2 Catalytic cracking.....	47
3.8.3 Hydrocracking.....	52
IV. EXPERIMENT STEUP.....	54
4.1 Raw material and Chemical.....	54
4.2 Apparatus and Instrument.....	54

CONTENTS (Continued)

CHAPTER	Page
4.2.1 The experimental unit.....	54
4.2.2 Vacuum pump.....	56
4.2.3 Gas chromatography (GC Simulated Distillation).....	56
4.2.4 Fourier-Transform Infrared Spectrometer (FTIR).....	56
4.3 Experimental Procedure.....	57
V. RESULTS AND DISCUSSIONS.....	59
Experimental Results.....	59
5.1 Influences of reaction temperature on composition of oil product.....	59
5.2 Influences of amount of catalyst on composition of oil product.....	63
5.3 Influences of reaction time on composition of oil product.....	65
5.4 Influences of initial pressure of hydrogen gas on composition of oil product.....	67
5.5 Characterization of functional groups of oil product by FT-IR.....	69
5.6 Comparison of this work with other work.....	72
VI. CONCLUSION AND RECOMMENDATION.....	74
REFERENCE.....	76
APPENDICE.....	79
APENDIX A. Data for study of product distribution from hydrocracking Of styrene-acrylonitrile copolymer on HZSM-5 catalyst.....	80
APENDIX B. Graph of product from gas chromatograph.....	85
VITA.....	99

LIST OF FIGURES

FIGURE	PAGE
3.1 SiO ₄ or AlO ₄ tetrahedron.....	20
3.2 Secondary building units(SBU's) found in the zeolite structures.....	21
3.3 Typical zeolite pore geometries.....	23
3.4 Small pore zeolite.....	24
3.5 Channel systems.....	25
3.6 Large pore zeolites.....	25
3.7 Sodalite cage structure.....	26
3.8 Perspective views of the faujasite structure.....	27
3.9 Diagram of the surface of a zeolite framework.....	35
3.10 Water molecules coordinate to polyvalent cation are dissociated by heat treatment yielding Bronsted acidity.....	36
3.11 Lewis acid site developed by dehydroxylation of Bronsted acid site.....	36
3.12 Steam dealumination process in zeolite.....	37
3.13 The enhancement of acid strength of OH group by their interaction with dislodge aluminum species.....	37
3.14 Diagram depicting the three type of selectivity.....	38
3.15 Correlation between pore size(s) of various zeolites and kinetic diameters of some molecules.....	43
4.1 The reaction experimental unit for conversion of SAN into oil products using HZSM-5 catalyst.....	55
4.2 The microreactor.....	55
4.3 Gas Chromatography (GC Simulated Distillation).....	56
4.4 The scheme of experiment in this research.....	58

LIST OF FIGURES (Continue)

FIGURE	PAGE
5.1 SAN conversion on HZSM-5 catalyst with various reaction temperatures.....	61
5.2 Gas yield of SAN on HZSM-5 catalyst with various reactions temperatures.....	62
5.3 SAN conversion on HZSM-5 catalyst with various weights of catalyst...	64
5.4 SAN conversion on HZSM-5 catalyst with various reaction time.....	66
5.5 SAN conversion on HZSM-5 catalyst with various initial hydrogen pressure.....	68
5.6 FT-IR spectrum of oil product	70
5.7 FT-IR spectrum of benzene oil octane number 95.....	70
B.1 Oil composition at condition 380 °C of reaction temperature, 200 psig of hydrogen, 60 min of reaction time and 2.5% of HZSM-5 catalyst by GC Simulated Distillation.....	87
B.2 Oil composition at condition 400 °C of reaction temperature, 200 psig of hydrogen, 60 min of reaction time and 2.5% of HZSM-5 catalyst by GC Simulated Distillation.....	88
B.3 Oil composition at condition 430 °C of reaction temperature, 200 psig of hydrogen, 60 min of reaction time and 2.5% of HZSM-5 catalyst by GC Simulated Distillation.....	89
B.4 Oil composition at condition 450 °C of reaction temperature, 200 psig of hydrogen, 60 min of reaction time and 2.5% of HZSM-5 catalyst by GC Simulated Distillation.....	90

LIST OF FIGURES (Continue)

FIGURE	PAGE
B.5 Oil composition at condition 0.5% of HZSM-5 catalyst, 430 °C of reaction temperature, 200 psig of hydrogen and 60 min of reaction time by GC Simulated Distillation.....	91
B.6 Oil composition at condition 1.25% of HZSM-5 catalyst, 430 °C of reaction temperature, 200 psig of hydrogen and 60 min of reaction time by GC Simulated Distillation.....	92
B.7 Oil composition at condition 30 min of reaction time, 430 °C of reaction temperature, 1.25% of HZSM-5 catalyst and 200 psig of hydrogen by GC Simulated Distillation.....	93
B.8 Oil composition at condition 90 min of reaction time, 430 °C of reaction temperature 1.25% of HZSM-5 catalyst, 200 psig of hydrogen and by GC Simulated Distillation.....	94
B.9 Oil composition at condition 100 psig of hydrogen, 430 °C of reaction temperature 1.25% of HZSM-5 catalyst and 60 min of reaction time by GC Simulated Distillation.....	95
B.10 Oil composition at condition 300 psig of hydrogen, 430 °C of reaction temperature, 1.25% of HZSM-5 catalyst and 60 min of reaction time by GC Simulated Distillation.....	96
B.11 Oil composition at condition 200 psig of hydrogen, 430 °C of reaction temperature, non-catalyst and 60 min of reaction time by GC Simulated Distillation.....	97
B.12 Oil composition at condition 430 °C of reaction temperature, 1.25% of HZSM-5 catalyst, non-hydrogen and 60 min of reaction time by GC Simulated Distillation.....	98

LIST OF TABLES

TABLE	PAGE
2.1 Properties of SAN copolymer.....	7
3.1 Zeolites and their secondary building units.....	21
3.2 Correlation between zeolites properties and catalytic functionality.....	29
3.3 Kinetic diameters of various molecules based on the Lennard-Jones Relationship.....	40
3.4 Shape of the pore mouth opening of known zeolite structures.....	41
5.1 Comparison of this with Kulwadee Pueaknapo.....	72
A-1 The condition reactions of all parameter for product distribution from hydrocracking of styrene-acrylonitrile copolymer on HZSM-5.....	81
A-2 The percentage of oil composition by GC Simulated Distillation.....	84


 สถาบันวิทยบริการ
 จุฬาลงกรณ์มหาวิทยาลัย

CHAPTER I

INTRODUCTION

Plastics have become a vital part of everyday life. The use of plastic materials is increasing rapidly year by year and in many applications they are replacing conventional materials such as metals, wood and natural fibers such as cotton and wool. Plastics are being produced and utilized worldwide at increasing rate in each subsequent year. Plastics are manufactured for various uses including, but not limited to, consumer packing, wires, pipes, containers, bottles, appliances, electrical/electronic part, and automotive parts.

Plastic can be made from chemical found in coal, gas or crude oil. Due to the limited of world's reserve of coal and crude oil, great effects are being made to find other carbon sources as feedstock materials for the production of fuels. The millions of tons of plastics into our dustbins every year. Most of this is buried in refuse sites along with our other rubbish. But, unlike wood or metals, plastics will remain there more or less forever as do not rot. This means that plastic rubbish remains unsightly. It also means that our valuable resources of oil are being wasted. But there are ways of reducing this wasted. Other plastics could be recycled. Thermoplastics could be melted down and re-used. Some plastic can be burned and used as a fuel to provide heat and power. The degradation of waste plastic into fuel represents a sustainable way, for the recovery of the addition to protecting the environment.

The amount of waste plastics is increasing all over the world. About 88% of waste plastics are disposed of in landfills or by combustion. Landfill and combustion is no longer acceptable for the disposal of plastics because of serious environmental

concerns and the low weight-to-volume ratio of plastics. Therefore, the recycling of waste plastics has received significant worldwide attention [1].

All waste materials are post-consumed since each has been used to some degree and has some level of contamination. Waste plastics may be contaminated with a variety of materials such as foodstuff, or detergent or motor oil, In addition, many different types of plastics are produced. Therefore, to recycle plastic waste to product fuels, the plastic materials must be carefully separated and cleaned so that only one type of plastic is present. Many plastics also contain inorganic that have been added to improve mechanical strength and thermal resistance or as flame retardant. Consequently, only a small amount of waste plastics is currently being recycled into fuels that can be used directly as recycled materials [2].

Therefore, this work aims to investigate the performances of the tested HZSM-5 zeolite catalyst on styrene acrylonitrile copolymer conversion to gasoline reaction.

The objectives of this research are:

- (1) To study the hydrocracking of styrene acrylonitrile copolymer (SAN) by uses HZSM-5 zeolite catalyst in microreactor.
- (2) To search for optimum conditions of cracking reaction to yield suitable percentage of products and composition.
- (3) To investigate and analyze oil products, conversion and products distribution produced from cracking.

The scopes of this research are:

- (1) Investigate the product distribution from hydrocracking of styrene acrylonitrile copolymer on HZSM-5 under the following conditions :
 - Reaction temperature range of 380-450°C
 - Quantity of catalyst as percent by weight range of 0-2.5%
 - Reaction time range of 30-90 min.
 - Pressure of hydrogen gas range of 0-300 psig
- (2) Analyzing fractions of oil product by GC Simulate Distillation.
- (3) Analyzing functional group of oil product by Fourier transform infrared spectroscopy.



สถาบันวิทยบริการ
จุฬาลงกรณ์มหาวิทยาลัย

CHAPTER II

LITERATURE REVIEW

Styrene Acrylonitrile Copolymer (SAN)

The name SAN copolymer is derived from polymerization process to styrene monomer and acrylonitrile monomer. SAN is a random amorphous copolymer of styrene and acrylonitrile. The commercial materials having an acrylonitrile content of 10-35%, usually in the range of 20-30%. They have better solvent resistance, higher impact strength and higher softening point than polystyrene, these properties improving as the acrylonitrile content increases. However their tendency to yellow and burn during processing also increases as the acrylonitrile content increases. Acrylonitrile is the more reactive monomer in copolymerization (the reactivity ratios being 0.4 and 0.04 for styrene and acrylonitrile respectively) and thus there is a tendency to alternation in the copolymers. Copolymers with much higher acrylonitrile contents (70%-80%) are often called high nitrile copolymer [3].

2.1 The Production of SAN Copolymer

SAN copolymer can be prepared from three polymerization processes: emulsion polymerization process, suspension polymerization process and bulk polymerization process.

2.1.1 Emulsion polymerization process

Emulsion polymerization is the process, which generally produces latexes. Here follows a description of the most general recipe to do an emulsion polymerization. An emulsion polymerization recipe starts with styrene monomer, acrylonitrile monomer, emulsifier and water. The monomer is an oily transparent substance, which is not very soluble in water the monomer is dispersed in the floating in it. Emulsifier molecules stabilize these monomer droplets.

2.1.2 Suspension polymerization process

The suspension polymerization recipe starts with styrene monomer, acrylonitrile monomer, suspending agent and water. In suspension polymerization there are two phases water and organic. SAN copolymer dissolved in the aqueous phase is a typical suspending agent.

The rate of suspension polymerization is similar to the rate of bulk polymerization but the heat transfer is much better for suspension polymerization.

2.1.3 Bulk polymerization process

In this process recipe starts with styrene monomer, acrylonitrile monomer with no water. Bulk polymerization has a built in hazard. The thermal conductivity of monomers and polymers is low, and as the viscosity builds up, the ability for heat

transfer *via* convection is substantially diminished. If the heat emergency cannot be dissipated, temperature rise and at higher temperatures the reaction is going to go faster, so this is a positive feedback loop with disastrous consequences.

For bulk polymerization removal of unreacted monomer can be a problem. This is a large concern if your safe polymer was prepared from monomers, which are toxic.

2.2 Physical and chemical properties

Commercial styrene acrylonitrile copolymer (SAN) typically contains approximately 76% styrene and 24% acrylonitrile. This material has a higher glass transition temperature and better impact strength than polystyrene [4].

To obtain a styrene based polymer of higher impact strength and higher heat distortion temperature at the same time, styrene is copolymerization with 20-30% acrylonitrile. Such copolymers have better chemical and solvent resistance and much better resistance to stress cracking and crazing while retaining the transparency of the homopolymer at the same time. In many respects SAN copolymers are also better than poly(methyl methacrylate) and cellulose acetate, two other transparent thermoplastics[5].

Compare properties with GPPS/SAN/PMMA

- | | |
|------------------------|-----------------|
| 1. Transparent | (PMMA>GPPS>SAN) |
| 2. Heat resistance | (PMMA/SAN>GPPS) |
| 3. Impact resistance | (PMMA>SAN>GPPS) |
| 4. Chemical resistance | (PMMA/SAN>GPPS) |
| 5. An easy processing | (GPPS>SAN>PMMA) |
| 6. Surface hardness | (PMMA>SAN>GPPS) |

The properties of SAN copolymer are shown in Table 2.1.

Table 2.1 Properties of SAN copolymer [6]

PROPERTY	SAN
<u>Physical Properties</u>	
Density (g/cc)	1.07-1.25
Water Absorption (%)	0.2-0.3
Linear Mold Shrinkage (cm/cm)	0.002-0.005
Melt Flow (g/10 min)	1.1-40
<u>Mechanical Properties</u>	
Tensile strength, Ultimate (Mpa)	45-84
Tensile modulus (Mpa)	3.3-4.1
Elongation at break (%)	1.5-7
Flexural Modulus (Gpa)	3.32-4.14
Izod Impact, Notched (J/cm)	0.11-0.267
Hardness, Rockwell M	83-85
Compressive Yield Strength (Mpa)	103-110
<u>Thermal Properties</u>	
Heat Capacity (J/g-°C)	1.2-2.23
Thermal Conductivity (W/m-k)	0.113-0.195
Deflection Temperature at 0.46 Mpa (°C)	96-110
Vicat Softening Point (°C)	103-120
Glass Temperature (°C)	120

2.3 Processing and application

The processing of SAN copolymer the material must be pre dried for all types of processing technology. A substantial proportion of the manufactured material is processed by injection moulding techniques. The temperature of the individual section in the injection moulding machine was varied from 193°C-288 °C and the melt polymer temperature was from 218 °C -260°C and the mould temperature was varied between 49°C -88°C

Extrusion is the second most widely used processing technology employed for SAN copolymer. Extrusion temperature usually varied between 177°C and 277°C the rear zone temperature is from 177°C -204°C. The middle zone temperature is from 210 °C -232°C and torpedo zone and die temperature is from 204°C -277°C

The main application of SAN copolymer depends on their good properties over a rigid, transparent, tough, resistant to greases, stress cracking and crazing, easily processed, heat resistant and chemical resistant.

SAN copolymer to be used in household product such as drinking tumblers, water jugs, toothbrush handles, kitchen and picnic ware. Electric appliances such as radio dials, TV set screens and auto part such as automotive instrument lenses and glass filled support panels.

2.4 Literature Reviews

Huffman *et al.*, [7] studied the investigations of the direct liquefaction reactions of waste plastics, medium and high density polyethylene (PE), polypropylene (PPE) and coal-plastic mixtures, varying the catalyst, temperature, gas, pressure, time and solvent. This experiment used four types of catalysts: a commercial HZSM-5 zeolite catalyst, and three catalysts synthesized in our laboratory, ferrihydrite treated with citric acid, coprecipitated $\text{Al}_2\text{O}_3\text{-SiO}_2$, and a ternary ferrihydrite- $\text{Al}_2\text{O}_3\text{-SiO}_2$. For direct liquefaction of plastics alone, a solid acid catalyst such as HZSM-5 or $\text{Al}_2\text{O}_3\text{-SiO}_2$ markedly improves oil and total liquid yields, as determined by pentane and THF solubility, respectively. Yields are higher when using either a waste oil solvent or no solvent than using tetralin as the solvent. For PE temperatures of 430 °C or higher are required for good yields, while PPE gives excellent yields at 420°C. A commingled plastic provided by the American Plastics Council (APC) exhibited peak oil and total liquid yields at 445-460°C. The oil yields and total liquid from PE (HZSM-5, 430°C) and the APC commingled waste plastic decreased only slightly with decreasing hydrogen pressure (from 800 to 100 psig H_2 (cold)). Furthermore, yields were as high under nitrogen (200-600 psig, cold) as under hydrogen.

Coliquefaction experiments were conducted on 50-50 mixtures of PE, PPE and the APC plastic with Black Thunder coal. For these experiments, the best results were obtained when the solvent was tetralin or mixture of tetralin and waste oil. Lower yields were observed with only waste oil or with no solvent. Either HZSM-5 or $\text{Al}_2\text{O}_3\text{-SiO}_2\text{-ferrihydrite}$ increased oil and total yields by approximately 10% at 460°C. Under the same condition yields from a PPE-coal mixture were substantially higher than those from a PE-coal mixture.

Aguado *et al.*, [8] studied the catalytic conversion of polyolefins into liquid fuels over MCM-41: comparison with ZSM-5 and amorphous $\text{SiO}_2\text{-Al}_2\text{O}_3$. The catalytic degradation of both low- and high-density polyethylene (LDPE and HDPE) and polypropylene (PP) has been investigated using MCM-41, a mesoporous aluminosilicates recently amorphous silica-alumina. For all the studied plastics, MCM-41 has been found more active than the amorphous $\text{SiO}_2\text{-Al}_2\text{O}_3$, as a consequence of the higher surface area and the uniform mesoporosity present in the former. Compared to ZSM-5, MCM-41 exhibits a lower activity for the degradation of linear and low branched polymers (HDPE and LDPE, respectively), which can be related to the higher strength of the zeolite acid sites. However, the opposite is observed for the cracking of highly substituted plastics such as PP due to the severe steric hindrances these molecules encounter to enter into the narrow pores of the zeolite, as confirmed by molecular simulation measurements. Moreover, for the cracking of LDPE, HDPE, and PP, the selectivity's toward hydrocarbons in the range of gasoline's and middle distillates obtained over MCM-41 are toward hydrocarbons in the range of gasoline and middle distillates obtained over MCM-41 are clearly higher than those of ZSM-5. Therefore, MCM-41 is a catalyst potentially interesting for the conversion of polyolefinic plastic wastes into liquid fuels.

Uemichi *et al.*, [9] studied the conversion of polyethylene into gasoline-range fuels by two-stage catalytic degradation using silica-alumina and HZSM-5 zeolite. A two-stage catalytic degradation of polyethylene using amorphous silica-alumina and HZSM-5 zeolite catalysts in series has been developed for converting the polymer into high-quality gasoline-range fuels. Compared with the one-stage degradation over each catalyst, the two-stage method provides some advantages. They are an improved gasoline yield and a high octane number despite low aromatics content. Significant results were obtained when silica-alumina and HZSM-5 were used in a weight ratio of 9:1 as upper and lower catalysts, respectively, in a flow reactor. The reverse sequence

of catalysts showed no advantage. It was suggested that large pores and moderate acidity of the silica-alumina loaded in the upper layer operated favorably to catalyze the degradation of polyethylene into liquid hydrocarbons. The resulting oils showed low quality, and they were transformed into high-quality gasoline on the strongly acidic sites of the HZSM-5 loaded in the lower layer at the expense of oil yield. Increases in concentration of isoparaffins and aromatics contributed to the upgrading.

Brebu *et al.*, [10] studied the composition of nitrogen-containing compounds in oil obtained from acrylonitrile-butadiene-styrene thermal degradation. The thermal degradation of the acrylonitrile-butadiene-styrene copolymer (ABS) was carried out at different temperatures from 360 to 440°C in static and dynamic atmospheres of nitrogen, using semibatch operation. Nitrogen-containing compounds were found in all three degradation fraction: gases (as NH₃ and HCN), oil, and residue. The percentage of the oil fraction increases with the increase of the degradation temperature. At 440°C 63 wt % of the initial ABS feed was recovered in the oil fraction. The nitrogen (N) concentration of the oil fraction was in the range of 29-40 mg/ml.

4-Phenylbutyronitrile is the main N-containing degradation product (16 -19 wt % in oil). N-compounds were also found as aliphatic and aromatic nitrile, amino derivatives, and heterocyclic compounds containing one or two N atoms such as pyridine, pyridine, and quinoline. Dynamic atmospheres of nitrogen and the residence time of the products in the reactor affects the oil recovery rate and the distribution of N in the degradation products.

Trisupakiti [11] studied the conversion of polyethylene into gasoline using HZSM-5 catalyst in a microreactor width of 30 mm inside diameter by varying operating conditions as pressure of hydrogen gas range of 10 to 30 kg/cm², reaction temperature range of 400 to 480 °C and reaction time range of 30 to 60 min for each catalyst. From the results, it was found that reaction temperature of 450 °C was the

temperature that yielded the highest quantity of oil product. This temperature was also used in studying the effect of pressure for hydrogen gas, reaction time and mole ratio Si/Al of HZSM-5 catalyst.

The analyzed oil product from Gas Chromatography (GC Simulated Distillation) was found that HZSM-5 was suitable and used as catalyst at 450 °C, hydrogen pressure at 30 kg/cm² and reaction 60 min. The product yield was in the range 20-45 % Naphtha, 8-16 % Kerosene, 9-16 % Gas Oil and 3-14 % Long Residues.

Pueaknapo [12] studied the conversion of acrylonitrile-butadiene-styrene (ABS) into oil product using iron on activated carbon catalyst. Experiment was done in a microreactor width of 30 mm inside diameter and volume of 70 ml by varied between 390 and 450°C, 20 to 40 kg/cm², respectively. While reaction time, amount of catalyst and percentages loading of iron were varied between 30 and 90 min, 0 and 0.75 g and 1, 5, 10 % on activated carbon catalyst, respectively.

The analyzed oil product from Gas Chromatography (GC Simulated Distillation) was found that iron on activated carbon catalyst was suitable to crack ABS. The optimum condition was 430°C, hydrogen pressure at 40 kg/cm², reaction time 60 min, amounts of catalyst was in the range of 45% naphtha, 4.8%kerosene, 8.1% gas oil and 9.1% long residues. Moreover, the product showed aromatic functional group, by means of Fourier Transform Infrared Spectrometer, which indicated the presence of high octane number and also showed low intensity of N-containing.

Brebu *et al.*, [13] studied the thermal and catalytic degradation of acrylonitrile-butadiene-styrene copolymer (ABS) was performed at 400 °C in static nitrogen atmosphere, by semibatch operation. γ -Fe₂O₃, a Fe₃O₄-C composite and α -FeOOH

were used as catalysts, in two contact modes: either mixed with the polymer or in contact with the volatile degradation products of ABS. All iron oxides decrease the concentration of nitrogen (N) in ABS degradation oil. Reactions in a flow-type reactor with 4-phenylbutyronitrile as model N-containing compound show that α -FeOOH is active at low temperatures (250-300°C) in converting heavy N-containing compounds into light aliphatic nitriles. XRD analysis proved that during reaction α -FeOOH was transformed into Fe_3O_4 in several steps, with α - Fe_2O_3 as intermediary compound.

Seo *et al.*, [14] studied the investigation of catalytic degradation of high density polyethylene by hydrocarbon group type analysis. Catalytic degradation of waste high-density polyethylene (HDPE) to hydrocarbons by ZSM-5, zeolite-Y, mordenite and amorphous silica-alumina were carried out in a batch reactor to investigate the cracking efficiency of catalysts by analyzing the oily products including paraffins, olefins, naphthenes and aromatics with gas chromatography/mass spectrometry (GC/MS). Catalytic degradation of HDPE with zeolite-Y, mordenite and amorphous silica-alumina yielded 71-82 wt % oil fraction, which mostly consisted of C6-C12 hydrocarbons, whereas ZSM-5 yielded much lower 35% oil fraction, which mostly consisted of C6-C12 hydrocarbons. Both all zeolites and silica-alumina increased olefin content in oil products and ZSM-5 and zeolite-Y particularly enhanced the formation of aromatics and branch hydrocarbons. ZSM-5 among zeolites showed the greatest catalytic activity on amount of coke. Amorphous silica-alumina also showed a great activity on cracking HDPE to lighter olefins in high yield, but no activity on aromatic formation.

CHAPTER III

THEORY

3.1 Introduction

Zeolites are a specific classification of microporous crystalline aluminosilicates frequently employed in catalysis. Zeolites are catalytic useful because they have a pores with a fixed dimension and volume. The crystalline pores have volumes approximately equal to many molecules used in catalytic processes. The fixed pore dimensions allow zeolites to use for specific applications. The primary applications for zeolites include catalytic cracking for gasoline products, ion exchange, gaseous filtration, and desiccants (removal of water vapor), and shape selective catalysis.

The primary building block of the zeolites is a SiO_4 tetrahedron structure. The SiO_4 tetrahedrons are combined through oxygen sharing to form individual silicate layers. When the tetrahedrons combined to form a ring consisting of five oxygen atoms, the structure is referred to as a pentasil. While there exist over 100 zeolites, one of the most well know zeolites is ZSM-5. The structure of ZSM-5 consists of neighboring layers being related through an inversion to develop a network of 10-membered rings. Aluminum atoms may replace the Si atoms in the matrix to develop a secondary building block frequently referred to as a truncated octahedron or a sodalite cage. The sodalite cages can be combined through shared square faces to form sodalite supercages. The sodalite supercages have pore large enough to contain a sphere with a diameter of 0.42nm. To increase the pore volume, the individual sodalite cages are commonly constructed through oxygen sharing between the four membered face to produce a structure called Zeolite A. Zeolite A has a considerably larger pore volume

and can accommodate a sphere with a diameter of 1.14nm. The most commonly used zeolite is the faujasite. Faujasite have a three-dimensional pore structure comprised of 12 membered oxygen rings capable of admitting hydrocarbon molecules larger than naphthalene. These zeolites are primarily used for the catalytic cracking of petroleum. The structure of faujasite is similar to that of Zeolite A, although the oxygen molecules are shared between the six membered faces and are capable of admitting a sphere with Zeolites possess a uniform pore volume distribution. As a result, pore volumes are used to classify individual zeolite structures. However, zeolites can be further grouped according to their composition, namely their Si/Al ratio. The Si/Al ratio is important because the ion exchange capacity is equal to the concentration of Al^{3+} cations. There are also correlation's between the acidic strength of the zeolite and the Si/Al ratio.

Zeolites are useful for selective catalysis because of their uniform pore volume distribution. The intrinsic pore volumes can control the selectivity of a catalytic reaction through transport or diffusional limitations, steric catalytic restrictions, and product trapping. The transport restrictions are dependent on the pore dimensions and molecule the catalytic size. The molecule may be too large to fit into the intrinsic pores, essentially blocking the catalytic sites. The pore volume may also limit the formation of intermediates or final products. In this instance, the desired isomer may be preferentially synthesized at high conversions and yields. Additionally, the pore volume may be large enough to contain the molecule, but the pore entrance may be too small to allow the molecule to diffuse out of the pores.

The acidic/basic nature of zeolites is also used for the catalytic cracking of petroleum. Zeolites can be formulated to have properties classified as a superacid. The acidic nature of the zeolites facilitates the low temperature cracking of larger hydrocarbon molecules (paraffins). However, catalytic cracking also produces several undesirable side reactions, including the formation of coke, a high molecular weight

aromatic. The coke deposits act as a poison, blocking the pore entrance and deactivating the zeolite. This complication is bypassed through the implementation of a fluidized bed reactor capable of catalyst regeneration [15].

3.2 History of Zeolites [11]

3.2.1 Previous history

The history of zeolites began in 1756 when the Swedish mineralogist Cronstedt discovered zeolite material, stilbite. He recognized zeolites as a new class of materials consisting of hydrated aluminosilicates of alkali and alkaline earths. Because the crystals exhibit swelling and boiling when heated in a blowpipe flame, Cronstedt called the mineral a "zeolite" derived from two Greek words, "zeo" and "lithos" meaning "to boil" and "a stone". In 1777 Fontana described the phenomenon of adsorption on charcoal. In 1840 Damour observed that crystals of zeolites could be reversibly dehydrated with no apparent change in their transparency or morphology. Schafhautele reported the hydrothermal synthesis of quartz in 1845 by heating "gel" silica with water in an autoclave. Way and Thompson (1850) clarified the nature of ion exchange in soils. Eichhom in 1858 showed the reversibility of ion exchange on zeolite materials. St. Clarife Deville reported the first hydrothermal synthesis of zeolite, Irbyniyr, in 1862. In 1866 Friedel developed the idea that structure of dehydrated zeolites consists of open spongy frameworks after observing that various liquids such as alcohol, benzene, and chloroform were occluded by dehydrated zeolites. Grandjean in 1909 observed that dehydrated chabazite adsorbs ammonia, air, hydrogen and other molecules, and in 1925 Weigel and Steinhoff reported the first molecular sieve effect. They noted that dehydrated chabazite crystal rapidly adsorbed water, methyl alcohol,

ethyl alcohol and formic acid but essentially excluded acetone, ether or benzene. In 1927 Leonard described the first use of x-ray diffraction for identification in mineral synthesis. The first structures of zeolites were determined in 1930 by Taylor and Pauling. In 1932 McBain established the term "molecular sieve" to define porous solid materials that act as sieves on a molecular scale.

Thus, by the mid-1930's the literature described the ion exchange, adsorption, molecular sieve and structural properties of zeolite minerals as well as a number of reported syntheses of zeolites. The latter early synthetic work remains unsubstantiated because of incomplete characterization and the difficulty of experimental reproducibility.

Barer began his pioneering work in zeolite adsorption and synthesis in the mid-1930's to 1940's. He presented the first classification of the known zeolites based on molecular size consideration in 1945 and in 1948 reported the first defined synthesis of zeolite including the synthetic analogue of the zeolite mineral merdenite.

3.2.2 Industrial history

3.2.2.1 Synthetic zeolites

Barrer's in the mid-late 1940's inspired the Linde Division of Union Carbide Corporation to initiate studies in zeolite synthesis in search of new approaches for separation and purification of air. Between 1949 and 1954 R.M. Milton and coworker D.W. Breck discovered a number of commercially significant zeolites, type A, X and Y. In 1954 Union Carbide commercialized synthetic zeolites as a new class of

industrial material for separation and purification. The earliest applications were the drying of refrigerant gas and nature gas. In 1959 a zeolite Y-based catalyst was marketed by Carbide as an isomerization catalyst.

In 1962 Mobil Oil introduced the use of synthetic of zeolite X as a cracking catalyst. In 1969 Grace described the first modification chemistry based on steaming zeolite Y to form an "ultrastable" Y. In 1967-1969 Mobil Oil reported the synthesis of the high silica zeolites beta and ZSM-5. In 1974 Henkel introduced zeolite A in detergents as a replacement for the enviromentally suspect phosphates. By 1977 industry-wide 22,000 tons of zeolite Y were in use in catalytic cracking. In 1977 Union Carbide introduced zeolite for ion-exchange separations.

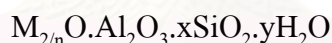
3.2.2.2 Natural zeolite

For 200 years following their discovery by Cronsted, zeolite minerals (or natural zeolite) were considered to occur typically as minor constituent in cavities in basaltic and volcanic rock. Such occurrences precluded their being obtained in mineable quantities for commercial use. From 1950 to 1962 major geologic discoveries revealed the widespread occurrence of a number of nature zeolite in sedimentary deposits throughout the Western United States. The discoveries resulted from the use of x-ray diffraction to examine very fine-grained (1-5 μm) sedimentary rock. Some zeolites occur in large near monomineralic deposits suitable for mining. Those that have been commercialized for adsorbent applications include chabazite, erionite, modemite and clinoptilolite.

3.3 Structure of Zeolite [16]

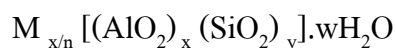
Zeolites are finding applications in many areas of catalysis and molecular sieve, generating interest in these materials in industrial and academic laboratories. As catalyst, zeolites exhibit appreciable acid activity with sharp-selectivity features not available in the compositional equivalent amorphous catalysts. In addition, these materials can act as supports for numerous catalytically active metals.

Zeolite Structurally, the zeolite is a crystalline aluminosilicates with a framework based on an extensive three-dimensional network of oxygen ions. Situated within the tetrahedral sites formed by the oxygen can be either a Si^{+4} or an Al^{+3} ion. The AlO_2^- tetrahedra in the structure determine the framework charge. This is balanced by cations that occupy nonframework positions. A representative empirical formula for a zeolite is written as:



M represents the exchangeable cations, generally from the group I or II ions, although other metal, nonmetal, and organic cations may also be used to balance the framework charge, and n represents the cation valence. These cations are present either during synthesis or through post-synthesis ion exchange. The value of x is equal to or greater than 2 because Al^{+3} does not occupy adjacent tetrahedral sites. The crystalline framework structure contains voids and channel of discrete size.

The structure formular of zeolite is based on the crystallographic unit cell, the smallest unit of structure, represented by:



Where n is the valence of cation M, w is the number of water molecules per unit cell, x and y are total number of tetrahedra per unit cell, and y/x is 10 to 100

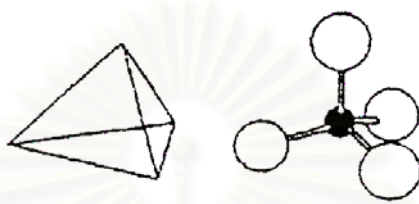


Figure 3.1 SiO₄ or AlO₄ tetrahedron [17].

In most zeolite structures the primary structural units, the AlO₄ or SiO₄ tetrahedra, are assembled into secondary building units (SBU). The final structure framework consists of assemblages of secondary units.

A secondary building unit consists of selected geometric groupings of those tetrahedra. There are nine such building units, which can be used to describe all of, know zeolite structures. These secondary building unit consist of 4, 6 and 8-member single ring, 4-4, 6-6, 8-8-remember double ring, and 4-1, 5-1, 4-4-1 branch ring. The topologies of these units are show in figure 3.2 Also listed are the symbols used to describe them. Most zeolite framework can be generated from several different SBU's. Descriptions of known zeolite structures based on their SBU's are listed in Table 3.1. Their 5-1 building units describe both zeolite ZSM-5 and ferrierite. Offertile, zeolite structure can be described by several units.

Table 3.1 (Continued)

Zeolite	Secondary Building Units								
	4	6	8	4-4	6-6	8-8	4-1	5-1	4-4-1
Sodalite X	X								
Henulandite									X
stibite								X	
Natrolite							X		
Thomsonite							X		
Edingtonite							X		
Cancrinite		X							
Zeolite L		X							
Mazzite X									
Merlinoite	X		X				X		
Phillipsite	X		X						
Losod		X							
Erionite X	X								
Paulingite	X								
Offretite		X							
TMA-E(AB)	X	X							
Gismondine	X		X						
Levyne		X							
ZK-5	X	X	X		X				
Chabazite	X	X			X				
Gmelinite	X	X	X		X				
Rho	X	X	X			X			
Type A	X	X	X	X					
Faujasite	X	X				X			

3.3.1 Pore size

All zeolites that are significant for catalytic and adsorbent applications can be classified by the number of T atoms, where T = Si or Al, that define the pore opening. There are only three pore openings known to date in the aluminosilicates zeolite system that are of practical interest for catalytic applications; they are descriptively referred to as the 8, 10 and 12 ring opening. Zeolites containing these pore openings may also be referred to as small (8-member ring), medium (10-member ring) and large (12-member ring) pore zeolites. Some typical pore geometries are shown in Figure 3.3[16].

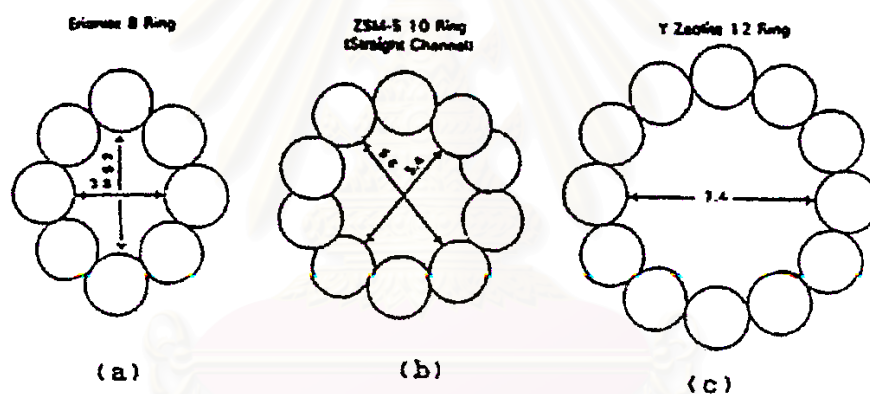


Figure 3.3 Typical zeolite pore geometries [16].

3.3.1.1 Small pore zeolite [11]

Structures of some small pore zeolite are illustrated in Figure 3.4. The erionite structure, Figure 3.4 (a), is hexagonal containing "supercage" supported by column of cancrinite units linked through double 6 rings. Access to and between, the supercages is gained through 8 rings.

In the chabazite framework, Figure 3.4 (b), the double rings layer sequence is ABCABC, and the 6 rings units are linked together through tilted 4 ring units. The framework contains large ellipsoidal cavities, Figure 3.4 (c), each entered through six 8 ring units, These cavities are joined via their 8 ring units, forming a 3 dimensional channel system.

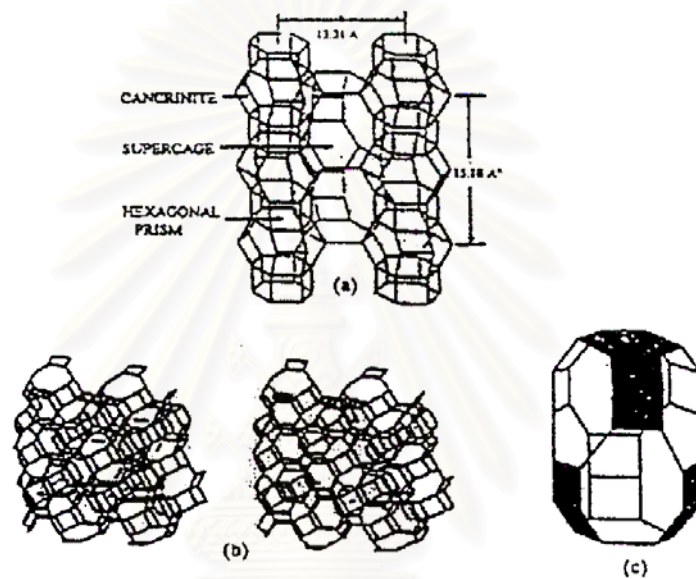


Figure 3.4 Small pore zeolite

(a) Erionite framework

(b) Chabazite framework

(c) Chabazite cavity [11]

3.3.1.2 Medium pore zeolites [11]

The channel system of zeolite ZSM-5, represented in Figure 3.5, shows a unique pore structure that consists of two intersecting channel systems: one straight ($5.5 \times 5.6 \text{ \AA}$) and other sinusoidal ($5.1 \times 5.4 \text{ \AA}$) and perpendicular to the former. Both channel systems have 10-membered ring elliptical openings.

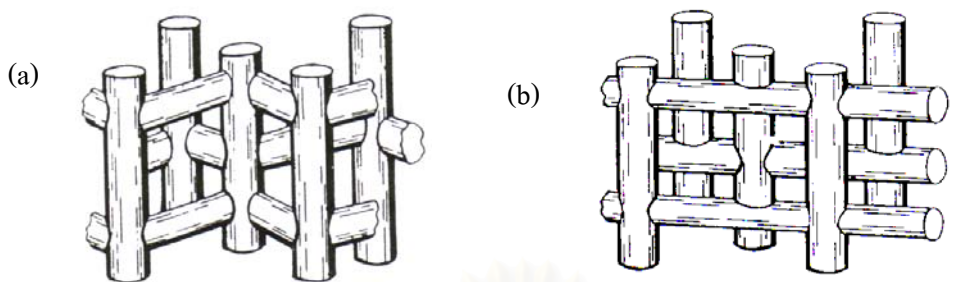


Figure 3.5 channel systems (a) ZSM-5 and (b) ZSM-11 [16].

3.3.1.3 Large pore zeolites [11]

Mordenite, Figure 3.6 (a), is characterized by a one-dimensional system of parallel elliptical channels, defined by 12-oxygen ring.

The faujasite structure, Figure 3.6 (b), is built up of truncated octahedron interconnected via double 6 ring units. Faujasite contains large supercages ($\sim 13 \text{ \AA}$ diameter) entered 12 oxygen ring.

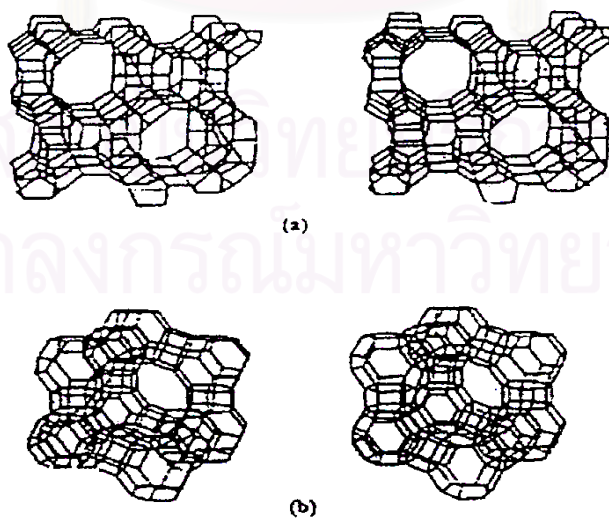


Figure 3.6 Large pore zeolites (a) Mordenite framework (b) Faujasite framework [11].

3.4 X and Y Zeolite Structures [18]

X zeolite, Y zeolite and faujasite have topologically similar structures. They differ in their characteristic silica-to-alumina ratios and consequently differ in their crystallattice parameter, with a variation of about 2 percent over the range of permissible Si/Al ratios. They also differ in properties as cation composition, cation location, cation exchangeability, thermal, adsorptive and catalytic character.

In the X and Y zeolites and faujasite, the silica and alumina tetrahedra are joined together to form a cuboctahedron, as show in figure 3.7. This unit referred to as a sodalite unit or truncated octahedron contains 24 silica and tetrahedra. The sodalite unit is the secondary building block of a number of zeolites, including sodalite, zeolite A, zeolite X, zeolite Y and faujasite. Molecules can penetrate into this unit through the six-membered oxygen rings, which have a free diameter 2.6 \AA , the unit contains spherical void volume with 6.6 \AA free diameter. Since the pore diameter is so small, only very small molecules, e.g., water, helium, hydrogen, or ions can enter the sodalite cage.

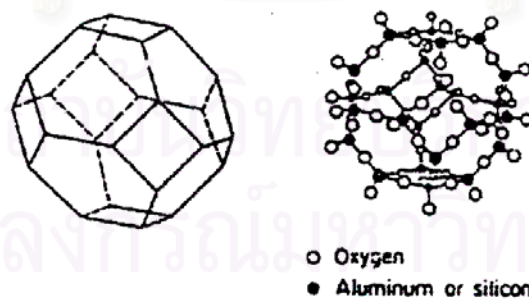


Figure 3.7 Sodalite cage structure. A formal representation of a truncated octahedron is shown on the left, and individual atoms are indicated on the right: the lines in the structure on the left represent oxygen anions, and the points of intersection represent silicon or aluminium ions [18].

The unit cell of faujasite-type zeolite is cubic with a unit-cell dimension of 25 \AA , and it contains 192 silica and alumina tetrahedra. The unit cell dimension varies with Si/Al ratio. Each sodalite unit in the structure is connected to four other sodalite units by six bridge oxygen ions connecting the hexagonal faces of two units, as shown in Figure 3.8. The truncated octahedra are stacked like carbon atom in diamond. The oxygen-bridging unit is referred to as a hexagonal prism, and it may be considered another secondary unit. This structure results in a supercage (sorption cavity) surrounded by 10 sodalite unit which is sufficient large for an inscribed sphere with a diameter of 12 \AA . The opening into this large cavity is bounded by 6 sodalite units, resulting in a 12 member oxygen ring with a 7.4 \AA free diameter. Each cavity is connected to four other cavities, which in turn are themselves connected to three additional cavities to form a highly porous framework structure.



Figure 3.8 Perspective views of the faujasite structure. The silicon or aluminium ions are located at the corner and the oxygen ions near the edges. Type I and II sites are indicated; the supercage is in the center [18].

This framework structure is the most open of any zeolite and is about 51 percent void volume, including the sodalite cage; the supercage volume represents 45 percent of the unit cell volume. The main pore structure is three-dimensional and large enough to admit large molecules, e.g., naphthalene and fluorinated hydrocarbon. It is

within the pore structure involving the sodalite unit exists but its apertures are too small to admit most molecules of interest in catalysis.

3.5 Zeolites as Catalysts [19]

The first use of zeolite as catalysts occurred in 1959 when zeolite Y was used as an isomerization catalyst by Union Carbide. More important was the use of zeolite X as a cracking catalyst in 1962, based upon earlier work by Plank and Rosinski. They noted that relatively small amounts of zeolites could be incorporated into the then standard silica/alumina or silica/clay catalysts. The use of zeolite in this way as promoters for petroleum cracking greatly improved their performance.

3.5.1 Potential versatility of zeolites as catalysts

Vaughan has graphically described zeolites as "molecules boxes" which have variable dimensions suited to the encouragement of molecular rearrangements inside their confined geometry. The conditions inside the "box", and box itself, can be controlled in a variety of ways based upon the unique properties of zeolite frameworks as summarized in Table 3.2

3.5.1.1 Crystal voidage and channels

Although some heterogenous reactions will take place at the external crystal surface, most practical zeolite catalysis takes places inside the framework. Here

zeolites have the advantage of vary large internal surface, about 20 times larger than their external surface for the more open framework (e.g. zeolite X and Y). This internal capacity provides the appropriate surfaces at which catalytic transformation can take place. In the faujasite zeolite is typically in the series of large cavities easily available via three-dimensional open-pore networks.

Further flexibility, which is useful for planned catalytic uses, arises in the more recently produced zeolites with subtle different cavity and channel systems. ZSM-5, for instance, has a three-dimensional system linked via intersections rather than cavities and mordenite catalysis seems to take place only in the largest channels.

Table 3.2 Correlation between zeolite properties and catalytic functionality [19].

Property	Catalytic Functionality
Crystal voidage and channels	An extensive internal surface to encourage catalytic processes.
Variable pore size	Creates both reactant and product selectivity via molecules sieving.
Ion exchange	Cation (I) control pore size, (ii) create high potential energy field within voidage (active site) and (iii) enable distribution of catalytically active metals on the zeolite substrate.
Salt occlusion	Controls pore size, provide another method of metal incorporation and can improve thermal stability and poisoning resistance.
Framework modification	Varies lattice change (by synthesis or modification) to enhance Active site production and thermal stability.

3.5.1.2 Variable pore sizes

Give that catalytic reaction takes place largely within zeolite framework, oxygen windows patently control access to this environment. This is diffusion-limited process, as is the effect of product molecules after transformations have taken place. This means that zeolites have very special practical advantages over the more traditional catalysts, in that admit only certain reactant molecules and this can be potentially tailored to produced selected product. This selectivity is know as "shapes selective catalysis" and controlled by "configurational diffusion" this phase was coined by Weiss to express a diffusion regiment in which useful catalytic reactions and promoted by virtue of a matching of size, shapes and orientation of the reactant product molecules to the geometry of zeolitic framework.

3.5.1.3 Ion exchange

Perhaps more relevant is the way in which ion exchange can be employed to place cations into very specific framework sites so as to create small volumes of high electrostatic filed. These fields are "active site" to which an organic reactant molecule can be attracted thus promoting the bond distortion and rupture essential to molecular rearrangements.

Another feature of ion exchange is that it provides a route for the introduction of metal cations with a view to their subsequent reduction to metal particles. These exist in the so-called "bifunctional" zeolite catalysts used to effect both hydrogenation and dehydrogenation reactions.

3.5.1.4 Salt occlusion

The introduction of a salt molecule into a zeolite can be first stage in the incorporation of a metal for subsequent reduction as mentioned above. It can also be used to enhance thermal stability. Yet another purpose is to "pacify" zeolite-cracking catalysts. The problem here is that crude oil contains metal cations (Ni, Cu, V, and Fe) originating from the metal porphyrins thought to play an inherent part in the geological formation of oil. These metals create unwanted reactivity causing carbon (coke) formation and subsequent loss of catalytic properties. The occlusive introduction of stannates, bismuthates, or antimonates pacifies these metals to extend useful catalyst bed life. It enables the refinery to cope with a variety of crude oil from different oil fields and illustrates the flexible technology, which can be achieved in zeolite catalysis.

Other salt treatments, via phosphates or fluorides, have been used to improve performance.

3.5.1.5 Framework modification

The electrostatic field of zeolite can be manipulated by isomorphous substitution into framework Si and Al sites. Synthetic or modification can do these routes. When the Si-Al ratio is close to 1 the field strength is at its highest as is the cation content- i.e. the conditions a greater separation of negative charge and hence higher field gradients (obviously also condition by cation position and cation types). In this way, the catalytic activity can be controlled, and parameters altered. A well known example of these effects is the way in which the thermal and chemical stabilities of synthetic faujasite can be critically altered by aluminium removal.

Framework substitution also can be created by the introduction of atoms other than Si and Al into tetrahedral sites via synthesis or modification. The ZSM-5 can accept B and Ga into tetrahedral sites by simple salt treatment as mentioned earlier, although a similar reaction in other frameworks is by no means as facile.

3.6 Zeolite Active sites

3.6.1 Acid sites [20]

Classical Bronsted and Lewis acid models of acidity are used to classify the active sites on zeolites. Bronsted acidity is proton donor activity; a tridiagonally coordinated alumina atom is an electron deficient and can accept an electron pair, therefore as a Lewis acid.

In general, the increase in Si/Al ratio will increase acidic strength and thermal stability of zeolite. Since the number of acidic OH groups depend on the number of aluminum zeolite's framework, decrease in Al content is expected to reduce catalytic activity of zeolite. If the effect of increase in the acidic centers, increase Al content, shall result in enhancement of catalytic activity.

Based on electrostatic consideration, the charge density at a cation site increases with increasing Si/Al. It was conceived that these phenomena are related to reduction of electrostatic interaction between framework sites, and possibly to difference in the order of aluminum in zeolite crystal-the location of Al in crystal structure.

Recently it has been reported the mean charge on proton was shifted regularly towards higher values as the Al content decreased. Simultaneously the total number of acidic hydroxyls, governed by the Al atoms, were decreased. This evidence emphasized that the entire acid strength distribution (weak, medium, and strong) was shifted towards stronger values. That is the weaker acid sites become stronger with the decrease in Al content.

An important in thermal and hydrothermal stability has been described to the lower density of hydroxyls groups, which is parallel to the Al content.

A longer distance between hydroxyl groups decreases the probability of dehydrogenation that generates defects on structure of zeolites.

3.6.2 Generation of acid centers [20]

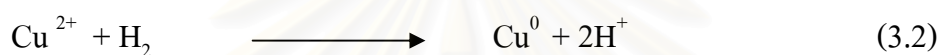
Protonic acid centers of zeolite are generated in various ways. Figure 3.9 depicts the thermal decomposition of ammonium exchange zeolites yielding the hydrogen form.

The Bronsted acidity due to water ionization on polyvalent cation, described below, is depicted in Figure 3.10.



The exchange of monovalent ions by polyvalent cations could improve the catalytic property. Those highly charged cations create very acidic centers by hydrolysis phenomena.

The Bronsted acid sites are also generated by the reduction of transition metal cations. The concentration of OH groups of zeolite containing transition metals was noted to increase by reduction with hydrogen at 250-450 ° C to increase with the rise of the reduction temperature.



The formation of Lewis acidity from Bronsted sites is depicted in Figure 3.12 [20]. The dehydration reaction decreases the number of protons and increases that of Lewis sites.

Bronsted (OH) and Lewis (-Al-) sites can be presented simultaneously in the structure of zeolite at high temperature. Dehydroxylation is thought to occur in ZSM-5 zeolite above 500°C and calcination at 800-900°C produces irreversible dehydroxylation that causes deflection in crystal structure of zeolite.

Dealumination is believed to occur during dehydroxylation, which may result from the steam generation within the sample. The dealumination is indicated by increases in the surface concentration of aluminum on the crystal. The dealumination process is expressed in Figure 3.12[20]. The extent of dealumination monotonously increases with the partial pressure of steam.

The enhancement of acid strength of OH group recently proposed to be pertinent to their interaction with those aluminum species sites tentatively expressed in Figure 3.13 [20]. Partial dealumination might therefore yield a catalyst of higher activity while severe steaming reduces the catalytic activity.

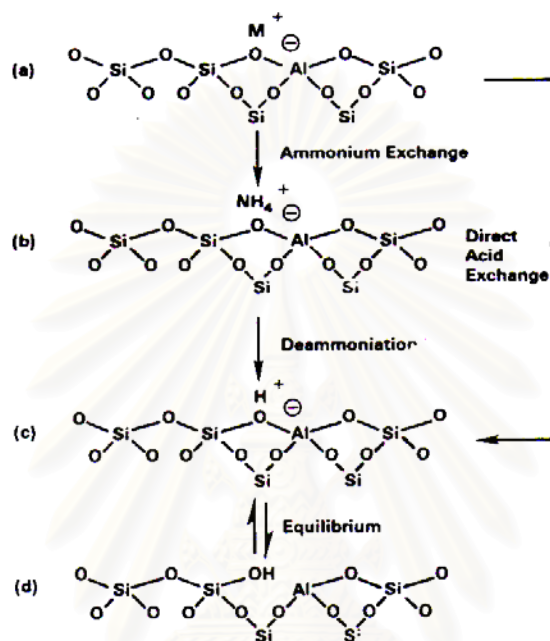


Figure 3.9 Diagram of the surface of a zeolite framework [20]

- (a) In the as synthesized form M^+ is either an ether and organic cation or an alkali metal cation.
- (b) Ammonium in exchange produces the NH_4^+ exchanged form.
- (c) Thermal treatment is used to remove ammonia, producing the H^+ , the acid form.
- (d) The acid form in (c) is in equilibrium with the form shown in (d), where there is a silanol group adjacent to a tricoordinate aluminium.

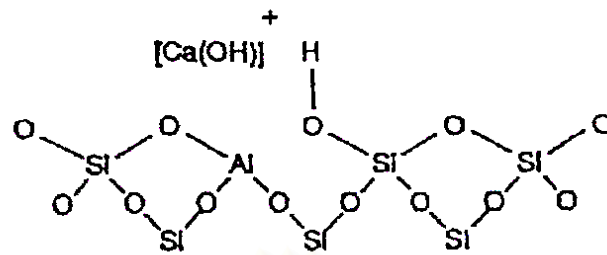


Figure 3.10 Water molecules coordinated to polyvalent cation are dissociated by heat treatment yielding Bronsted acidity[20].

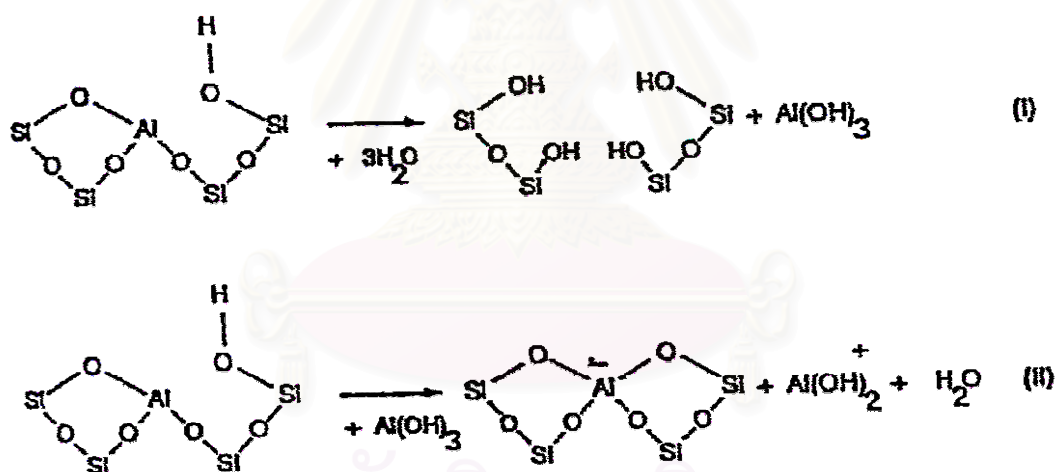


Figure 3.11 Lewis acid site developed by dehydroxylation of Bronsted acid site [20].

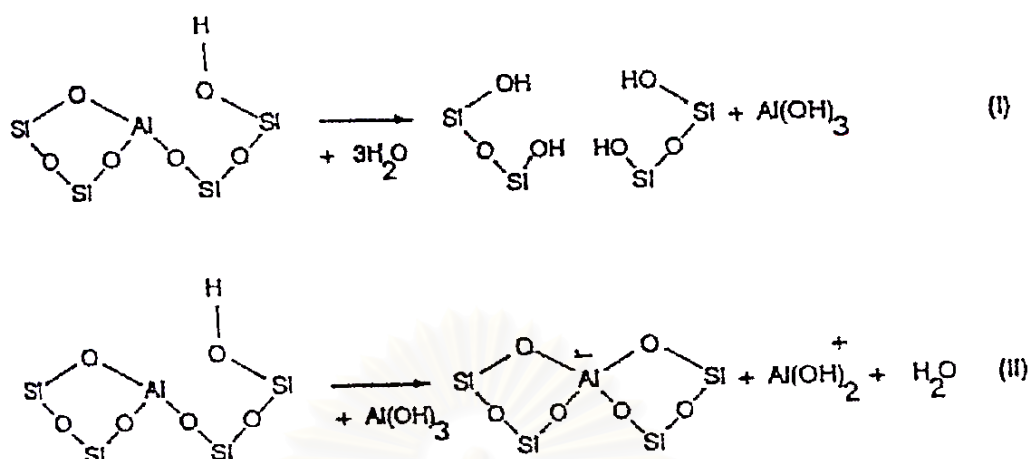


Figure 3.12 Steam dealumination process in zeolite [20].

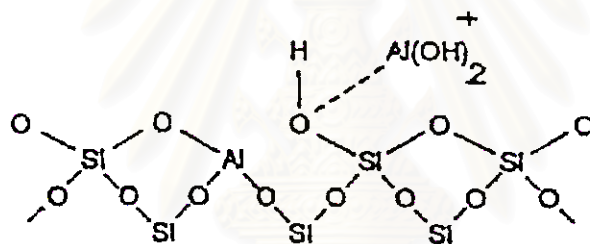


Figure 3.13 The enhancement of acid strength of OH group by their interaction with dislodge aluminum species [20].

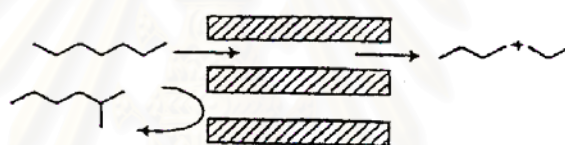
3.6.3 Basic sites

In certain instance reaction have been shows to be catalyzed at basic (cation) sites in zeolite without any influence from acid sites. The best characterized example of this is that of K-Y which splits n-hexane isomers at 500 °C. The potassium cations have been shown to control the unimolecular cracking (β -scission). Free radical mechanisms also contribute to surface catalytic reactions in these studies [11].

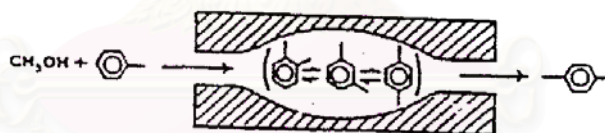
3.7 Shape-Selectivity Catalysis [20]

Many reaction involving carbonium ions intermediates are catalyzed by acidic zeolites. With respect to a chemical standpoint the reaction mechanisms are not fundamentally different with zeolite or with any other acidic oxides. What zeolite adds is shape selectivity effect. The shape selectivity characteristics of zeolites influence their catalytic phenomena by three modes; reactant shape selectivity, product shape selectivity and transition state shape selectivity. These types of selectivity are depicted in Figure 3.14 [20].

a) Reactant selectivity



b) Product selectivity



c) Transition state selectivity

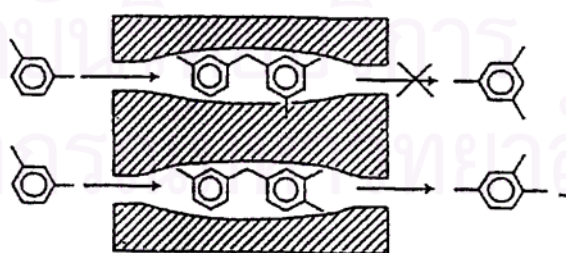


Figure 3.14 Diagram depicting the three type of selectivity [20].

Reactant or change selectivity results from the limited diffusibility of some of the reactants, which cannot effectively enter and diffuse inside crystal pore structures of the zeolites.

Product shape selectivity occurs as slowly diffusing product molecules cannot escape from the crystal and undergo secondary reactions. This reaction path is established by monitoring changes in product distribution as a function of varying contact time.

Restricted transition state shape selectivity is a kinetic effect arising from local environment around the active site, the rate constant for a reaction mechanism is reduced if the space required for formation of necessary state is restricted.

The critical diameter (as opposed to the length) of the molecules and the pore channel diameter of zeolite are important in predicting shape selective effects. However, molecules are deferrable and can pass through openings, which are smaller than their critical diameters. Hence, not only size but also the dynamics and structure of molecules must be taken into account.

Table 3.3 [20] presents values of selected critical molecular diameters and Table 3.4[16] presents values of the effective pore size of various zeolites. Correlation between pore size(s) and kinetic diameter of some molecules is depicted in Figure 3.15 [20].

Table 3.3 Kinetic diameters of various molecules based on the Lennard-Jones Relationship [20].

	Kinetic Diameter (Angstroms)
He	2.60
H ₂	2.89
O ₂	3.46
N ₂	3.64
NO	3.17
CO	3.76
CO ₂	3.30
H ₂ O	2.65
NH ₃	2.60
CH ₄	3.80
C ₂ H ₂	3.30
C ₂ H ₄	3.90
C ₃ H ₈	4.30
<i>n</i> -C ₄ H ₁₀	4.30
Cyclopropane	4.32
<i>i</i> -C ₄ H ₁₀	5.00
<i>n</i> -C ₅ H ₁₂	4.90
SF ₆	5.50
Neopentane	6.20
(C ₄ F ₉) ₃ N	10.20
Benzene	5.85
Cyclohexane	6.00
<i>m</i> -xylene	7.10
<i>p</i> -xylene	6.75
1,3,5 trimethylbenzene	8.50
1,3,5 triethylbenzene	9.20
1,3 diethylenebenzene	7.40
1-methylnaphthalene	7.90
(C ₄ H ₉) ₃ N	8.10

Table 3.4 Shape of the pore mouth opening of known zeolite structures.

The dimensions are based on two parameters, The T atom forming the channel opening (8, 10 12 ring) and the crystallographic free diameters of the channels. The channels are parallel to the crystallographic axis shown in brackets (e.g.<001>) [16].

STRUCTURE	8-MEMBER RING	10-MEMBER RING	12-MEMBER RING
Bikitaite	3.2 x 4.9[001]		
Brewsterite	2.3 x 5.0[100] 2.7 x 4.1[001]		
Cancrinite			6.2[001]
Chabazite	3.6 x 3.7[001]		
Dachiardite	3.6 x 4.8[001]	3.7 x 6.7[010]	
TMA-E	3.7 x 4.8[001]		
Edingtonite	3.5 x 3.9[110]		
Epistibite	3.7 x 4.4[001]	3.2 x 5.3[100]	
Erionite	3.6 x 5.2[001]		
Faujasite			7.4<111>
Ferrierite	3.4 x 4.8[010]	4.3 x 5.5[001]	
Gismondine	3.1 x 4.4[100] 2.8 x 4.9[010]		
Gmelinite	3.6 x 3.9[001]		7.0[001]
Heulandite	4.0 x 5.5[100] 4.1 x 4.7[001]	4.4 x 7.2[001]	
ZK-5	3.9<100>		
Luamontite		4.0 x 5.6[100]	
Levyne	3.3 x 5.3[001]		
Type A	4.1<100>		
Type L			7.1[001]

Table 3.4 (Continue)

STRUCTURE	8-MEMBER RING	10-MEMBER RING	12-MEMBER RING
Mazzite			7.4[001]
ZSM-11		5.1 x 5.5[100]	
Merlinoite	3.1 x 3.5[100] 3.5 x 3.5[010] 3.4 x 5.1[001] 3.3 x 3.3[001]		
ZSM-5		5.4 x 5.6[010] 5.1 x 5.5[100]	
Mordenite	2.9 x 5.7[010]		6.7 x 7.0[001]
Natrolite	2.6 x 3.9<101>		
Offretite	3.6 x 5.2[001]		6.4[001]
Paulingite	3.9<100>		
Phillipsitr	4.2 x 4.4[100] 2.8 x 4.8[010] 3.3[001]		
Rho	3.9 x 5.1<100>		
Stilbite	2.7 x 5.7[101]	4.1 x 6.2[100]	
Thomsonite	2.6 x 3.9[101] 2.6 x 3.9[010]		
Yugawaralite	3.1 x 3.5[100] 3.2 x 3.3[001]		

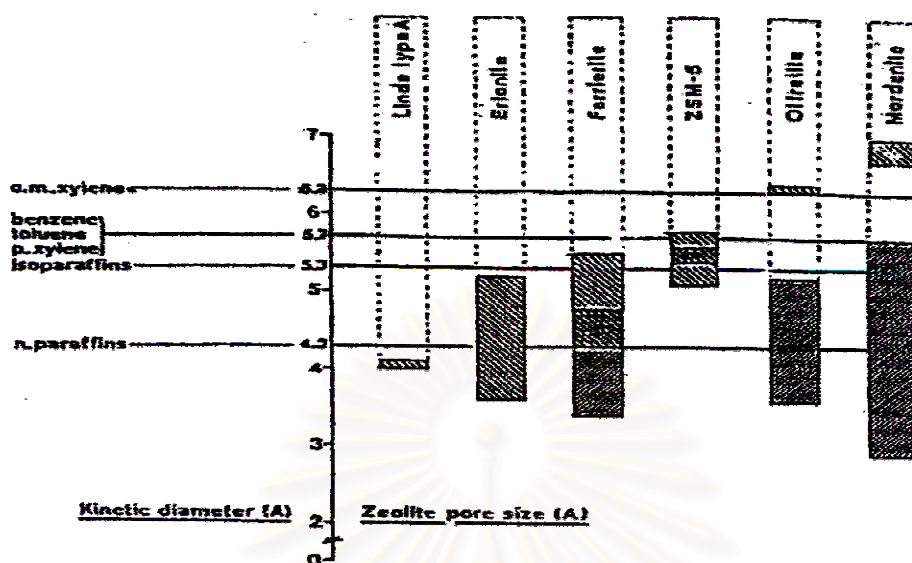


Figure 3.15 Correlative between pore size(s) of various zeolites and kinetic diameters of some molecules [20].

3.8 Mechanism of Cracking Processes

Cracking processes were assigned to three fundamental classes:

3.8.1 Thermal cracking [11, 21]

Thermal cracking, where free radicals (lacking one hydrogen atom on carbon atom in the hydrocarbon molecule) are intermediate species which cracked by a β -scission mechanism.

The most successful present explanation of thermal cracking of hydrocarbon is Rice free radical theory as modified by Kossiakoff and Rick. This will be called the "RK-theory" as follows to explain the cracking of normal paraffin:

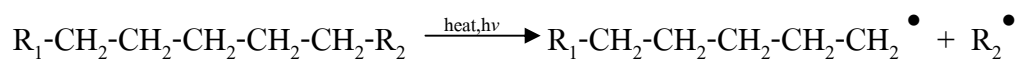
The normal paraffin molecule loses a hydrogen atom by collision and reaction with a small free hydrocarbon radical or a free hydrogen atom, there becoming a free radical itself. This radical may immediately crack or may undergo radical isomerization prior to cracking. Radical isomerization presumably occurs through a coiled configuration of a single radical, in which the hydrogen donor and acceptor carbon atom much closely approaches each other. Radical isomerization is a change of the position of hydrogen atom, usually to yield a more stable radical in order of tertiary > secondary > primary free radical.

Cracking of either the original or isomerized radical then take place at a carbon-carbon bond located in the β position to the carbon atom lacking one hydrogen atom. Cracking at the β position gives directly an alpha olefin and a primary radical (lacking one hydrogen atom on primary carbon atom); in this step no change of position of any hydrogen atom with respect to the carbon skeleton.

The primary radical derived from this step may immediately recrack at the β bond to give ethylene and another primary radical, or it may first isomerize. In the absence of radical isomerization, only primary radicals are derived from cracking reaction of normal paraffin; primary radicals are derived from cracking reaction of normal paraffin; primary radicals thus give only ethylene as the olefin product. By successive recracking, the radicals ultimately are reduced to methyl or ethyl fragments. These radicals then react with feedstock molecules to produce new free radicals and are themselves converted to methane or ethane. Thus, cracking is propagated as chain reaction.

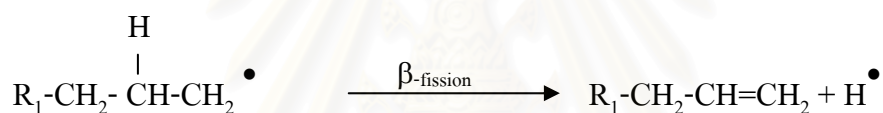
An example schematic representation of polyolefins cracking is as follows;

1. Initiation Step

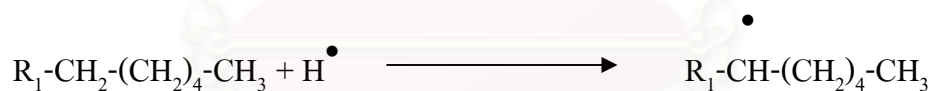


2. Propagation Step

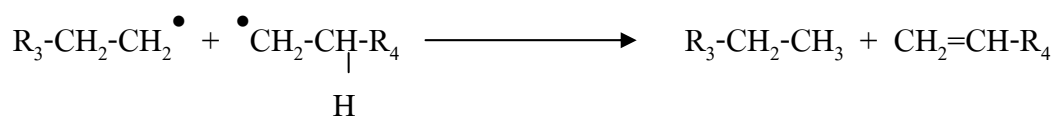
2.1 β -fission



2.2. Chain transfer

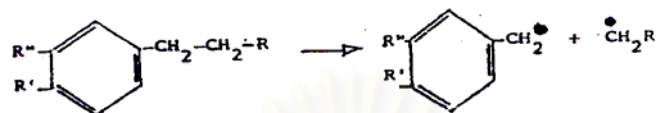


3. Termination Step

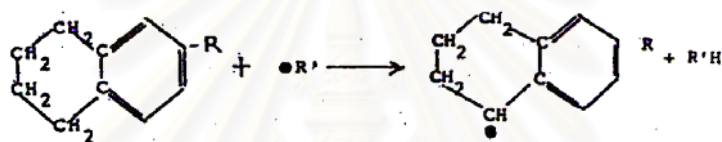


An example schematic representation of aromatic cracking is as follows:

1. Initiation Step

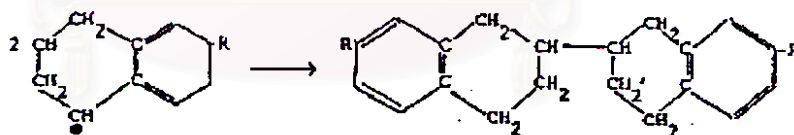


2. Chain Transfer

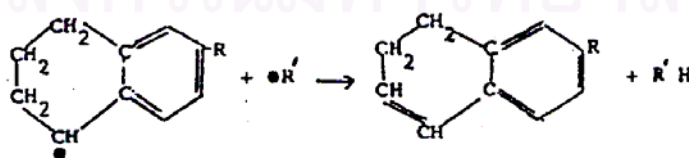


3. Termination

Coupling



Disproportionation



3.8.2 Catalytic cracking [11]

Catalytic cracking is the most important and widely used refinery process for converting heavy oil into more valuable gasoline and lighter product. Originally cracking was accomplished thermally but the catalytic process has almost completely replaced thermal cracking because of more gasoline having a higher octane and less heavy oil and unsaturated gases are produced.

Commercial cracking catalysts can be divided into three classes:

1. Acid-treated natural aluminosilicates
2. Amorphous synthetic silica-alumina
3. Crystalline synthetic silica-alumina catalysts called zeolites or molecular sieves.

Most catalysts used in commercial units today are either class (3) or mixtures of classes (2) and (3) catalysts. The advantages of the zeolite catalysts over the natural and synthetic amorphous catalysts are:

1. Higher activity
2. Higher gasoline yields at a given conversion
3. Product of gasoline containing a larger percentage of paraffin and aromatic hydrocarbons
4. Lower coke yield
5. Increased isobutane production

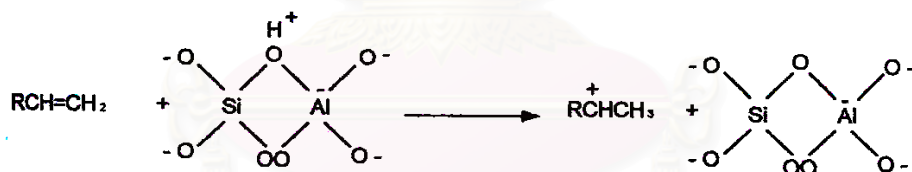
A major difference between thermal and catalytic cracking is that reactions through catalytic cracking occur via carbonium ion intermediate, compared to the free radical intermediate in thermal cracking. Carbonium Ions are longer-lived and

accordingly more selective than free radicals. Acid catalysts such as amorphous silica-alumina and crystalline zeolites promote the formation of carbonium ions. The following illustrates the different ways by which carbonium ions may be generated in the reactor:

1. Abstraction of a hydride ion by a Lewis acid site from a hydrocarbon



2. Reaction between a Bronsted acid site (H^+) and an olefin



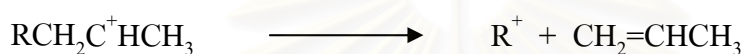
2. Reaction of a carbonium ion formed from step 1 or 2 with another hydrocarbon by abstraction of a hydride ion



Abstraction of a hydride ion from a tertiary carbon is easier than from a secondary, which is easier than from a primary position. The formed carbonium ion can rearrange through a methide-hydride shift similar to what has been explained in

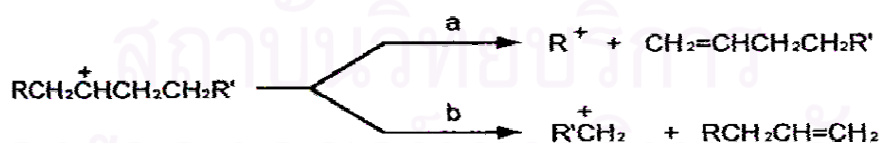
catalytic reforming. This isomerization reaction is responsible for a high ratio of branched isomers in the products.

The most important cracking reaction, however, is the carbon-carbon β bond scission. A bond at a position beta to the positively charged carbon breaks heterolytically, yielding an olefin and another carbonium ion. This can be represented by the following example:

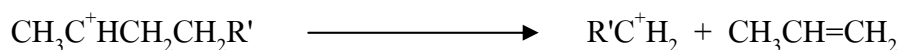


The new carbonium ion may experience another β scission, rearrange to a more stable carbonium ion, or react with a hydrocarbon molecule in the mixture and produce paraffin.

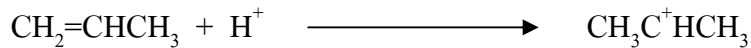
The Car-carbon β scission may occur on either side of the carbonium ion, with the smallest fragment usually containing at least three carbon atoms. For example, cracking a secondary carbonium ion formed from long chain paraffin could be represented as follows:



If $\text{R}=\text{H}$ in the above example, then according to the β scission rule (an empirical rule) only route becomes possible, and propylene would be a product:



The propene may be protonated to an isopropyl carbonium ion:



An isopropyl carbonium ion cannot experience β fission (no C-C bond β to the carbon with the positive charge). It may either abstract a hydride ion from another hydrocarbon, yielding propane, or revert back to propene by eliminating a proton. This could explain the relatively higher yield of propene from catalytic cracking units than from thermal cracking units.

Aromatization of paraffins can occur through a dehydrocyclization reaction. Olefinic compounds formed by the β scission can form a carbonium ion intermediate with the configuration conducive to cyclization. For example, if a carbonium ion such as that shown below is formed (by any of the methods mentioned earlier), cyclization is likely to occur.



Once cyclization has occurred, the formed carbonium ion loses a proton, and a cyclohexene derivative is obtained. This reaction is aided by the presence of an olefin in the vicinity ($\text{R}-\text{CH}=\text{CH}_2$).



The next step is the abstraction of a hydride ion by a Lewis acid site from the zeolite surface to form the more stable allylic carbonium ion. This is again followed by



proton elimination to form a cyclohexadiene intermediate. The same sequence is followed by a proton elimination to form a cyclohexadiene intermediate. The same sequence is followed until the ring is completely aromatized.

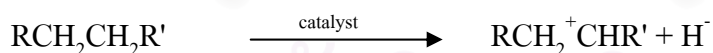
During the cracking process, Fragmentation of complex polynuclear cyclic compounds may occur, leading to formation of simple cycloparaffins. These compounds can be a source of C6, C7 and C8 aromatic through isomerization and hydrogen transfer reactions.

Coke formed on the catalyst surface is thought to be due to polycondensation of aromatic nuclei. The reaction can also occur through a carbonium ion intermediate of the benzene ring. The polynuclear aromatic structure has a high C/H ratio.

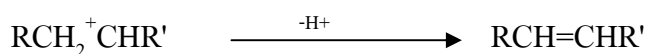
3.8.3 Hydrocracking [12]

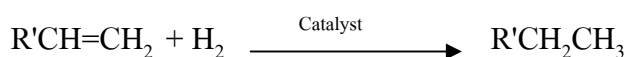
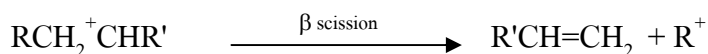
Hydrocracking is essentially catalytic cracking in the presence of hydrogen. It is one of the most versatile petroleum refining schemes adapted to process low value stocks. Generally, the feedstocks are not suitable for catalytic cracking because of their high metal, sulfur, nitrogen, and asphaltene. The process can also use feeds with high aromatic content.

The dual-function catalysts used in hydrocracking provide high surface area cracking sites and hydrogenation-dehydrogenation sites. Catalysts with strong acidic activity promote isomerization, leading to a high iso/normal ratios. Catalysts such as cobalt, molybdenum, tungsten, vanadium, palladium, or rare earth elements, on the other hand, provide the hydrogenation-dehydrogenation activity. As with catalytic cracking, the main reactions occur by carbonium ion and beta scission, yielding two fragments that could be hydrogenated on the catalyst surface. The main hydrocracking reaction could be illustrated by the first step formation of a carbonium ion over the catalyst surface:



The carbonium ion may rearrange, eliminate a proton to produce an olefin, or crack at a beta position to yield an olefin a new carbonium ion. Under an atmosphere of hydrogen and in the presence of a catalyst with hydrogenation-dehydrogenation activity, the olefins are hydrogenated to paraffinic compounds. This reaction sequence could be represented as follows:





As can be anticipated, most products from hydrocracking are saturated. For this reason, gasoline from hydrocracking units have lower octane ratings than those produced by catalytic cracking units; they have a lower aromatic content due to high hydrogenation activity. Products from hydrocracking units are suitable for jet fuel use. Hydrocracking also produces light hydrocarbon gasses (LPG) suitable as petrochemical feedstock.

Other reactions that occur during hydrocracking are the fragmentation followed by hydrogenation (hydrogenolysis) of the complex asphaltenes and heterocyclic compounds normally present in the feeds.

Hydrocracking reaction conditions vary widely, depending on the feed and the required products. Temperature and pressure range from 400 to 480⁰C and 35 to 170 atmospheres, respectively. Space velocities in the range of 0.5 to 2.0 hr⁻¹ are applied.

สถาบันวิทยบริการ
จุฬาลงกรณ์มหาวิทยาลัย

CHAPTER IV

EXPERIMENTAL SETUP

4.1 Raw Material and Chemical

The styrene-acrylonitrile copolymer (SAN) used in experiments is commercial grade supplied from Thai Petrochemical Industry Public Company Limited. It was virgin plastic of 3x3x2 mm size granules. The ratio of styrene and acrylonitrile is 76% and 24%, respectively. The catalyst used in this study as well commercial grade. Hydrogen gas (purity 99.5% minimum) and toluene (commercial grade; purity 80% minimum) were used as chemical reagents. Carbondisulfide (AR grade) was used as solvent for GC Simulate Distillation.

4.2 Apparatus and Instrument

4.2.1 The experimental unit

A microreactor (shown in **figure 4.1**) was used to carry out the reaction of styrene-acrylonitrile copolymer (SAN) with HZSM-5. The microreactor is stainless steel tube (SS.316) with an inner volume of 70 cm³ (shown in **figure 4.2**). It was heated by 450-watt electricity. The temperature was measured by thermocouple type R having 1.6-mm diameter with an accuracy of $\pm 5^{\circ}\text{C}$ by means of a programmable temperature controller. A speed motor was used to control the shaking of microreactor.

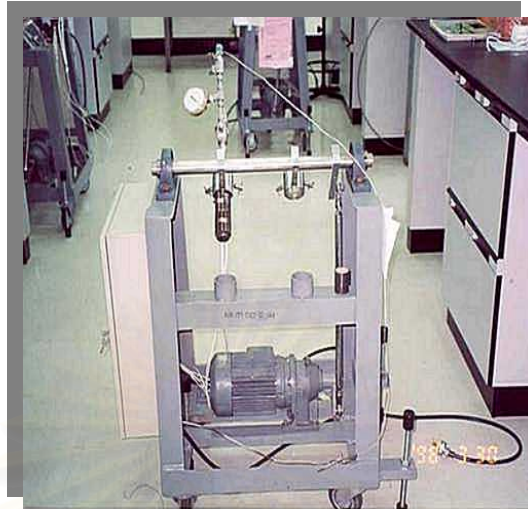


Figure 4.1 The reaction experimental unit for conversion of SAN into oil products using HZSM-5 catalyst.



Figure 4.2 The microreactor

4.2.2 Vacuum pump

The separation of liquid oil from catalyst and residue by using the vacuum filter pressure 1 kg/cm^2 .

4.2.3 Gas chromatography (GC Simulated Distillation)

The boiling range distribution is simulated by gas chromatograph (GC Simulated Distillation) as shown in **figure 4.3** for naphtha (IBP- 200°C), kerosene ($200\text{-}250^\circ\text{C}$), gas oil ($250\text{-}350^\circ\text{C}$), and long residue (up to 350°C) [23].



Figure 4.3 Gas chromatography (GC Simulated Distillation)

4.2.4 Fourier-Transform Infrared Spectrometer (FTIR)

FTIR, Perkin Elmer and model 1760, at Thai Petrochemical Industry Public Company Limited (TPI) was used to analyze the functional group of oil products.

4.3 Experimental Procedure

A 20 g of SAN and a required amount of catalyst were fed in a 70 ml microreactor under hydrogen atmosphere. Heating coil, insulator, and thermocouple were covered the reactor. The reactor was fixed with a shaker at 120 rpm for a required time reaction. After the reaction was ceased, the reactor was cooled down to room temperature. The liquid product was filtered. The oil composition was analyzed by distillation gas chromatograph. And the functional grouped was analyzed by Fourier transform infrared spectrometer. Toluene was used to dissolve the remaining product in the reactor. The experimental scheme was shown in **figure 4.4**.



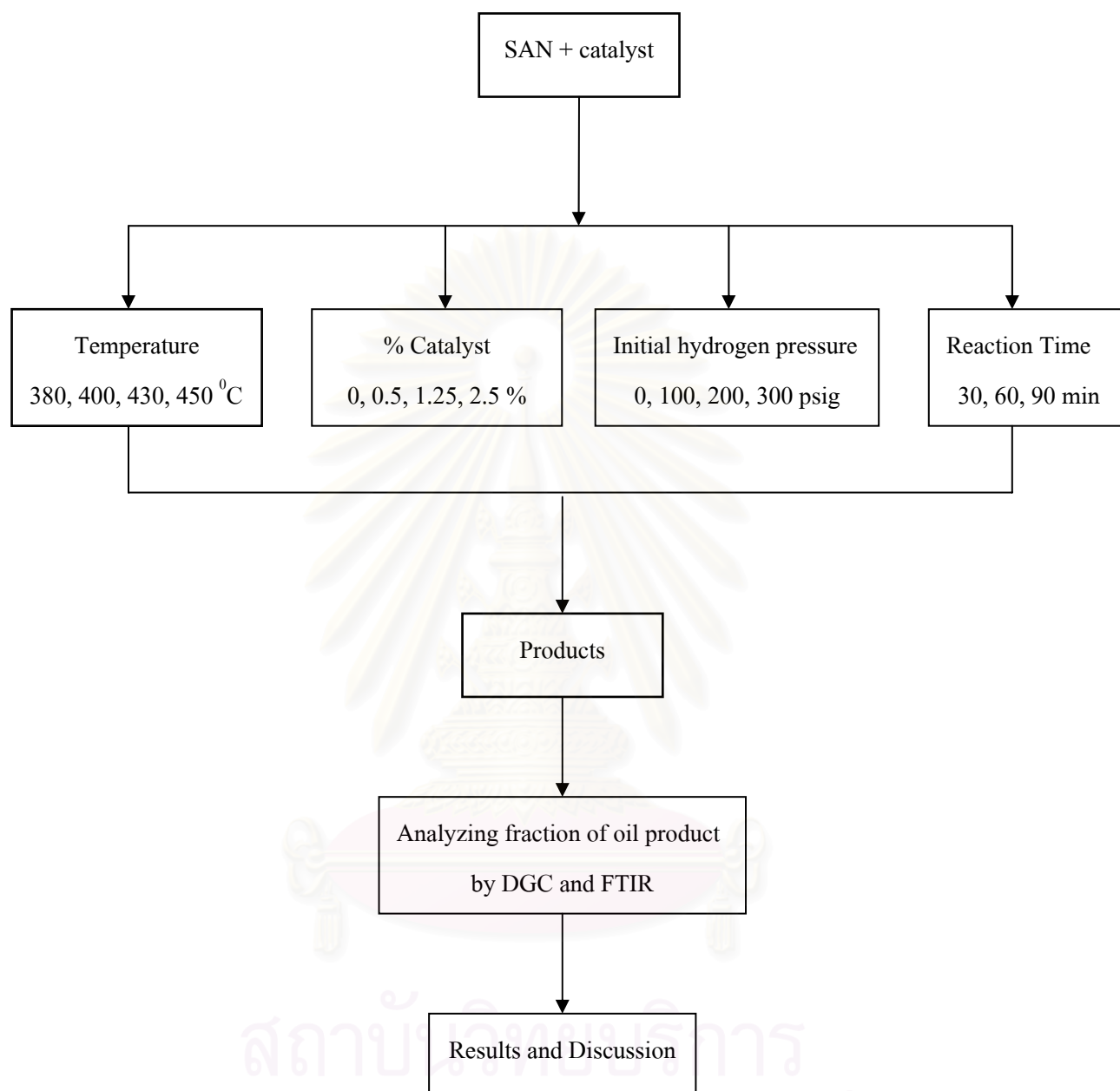


Figure 4.4 The scheme of experiment in this research.

CHAPTER V

RESULTS AND DISCUSSIONS

Experimental Results

The experimental results of styrene-acrylonitrile copolymer (SAN) hydrocracking by HZSM-5 catalyst were obtained by investigated its influences on percentage conversion of the products. The interested variables were temperature, ratio of styrene acrylonitrile copolymer (SAN) and catalyst, initial pressure of hydrogen gas and reaction time. Results are illustrated in **table A-1** and **A-2**. The influences of each variable mentioned above are shown in **figures 5.1-5.7**, respectively.

5.1 Influences of reaction temperature on composition of oil product

The influences of reaction temperature on the cracking of used styrene acrylonitrile copolymer (SAN) were performed by varied reaction temperatures of 380, 400, 430 and 450°C. Amount of HZSM-5 catalyst fixed at 2.5%, 200 psig initial hydrogen pressure and reaction time 60 min, respectively.

Generally, at reaction temperature lower than 380°C the produced were mainly the mixture of oil and wax. At temperature higher than 450°C wax could be further cracked resulting in a deposit of and solid at the surface of catalyst. Therefore, the experiment was carried out at reaction temperature 380, 400, 430 and 450°C only. The percentage of oil fraction from cracking was shown in **figure 5.1**. It shows that the percentage of oil yield product and naphtha increased from 56.79 to 78.02%, 24.25 to

34.06%, respectively. However, it observed that solid decreased from 42.11 to 20.79% when temperature increased from 380 to 400°C. It was noticed that at 430°C naphtha yield was more than those of 400°C about 5%. It can be pointed out that low reaction temperature was not suitable to crack SAN copolymer because of existing mixture of oil and wax product. It also showed that thermal cracking at low temperature was not able to break down SAN copolymer to lower hydrocarbon. At higher temperature (430°C), the thermal cracking was accelerated converting SAN to kerosene and gas oil. The kerosene and gas oil was catalytically cracked at the surface of HZSM-5 to naphtha and gases (normally C₁-C₄). On the contrary, it was found that total solid increased about 6% at surface of catalyst, which means that coking, occurred at the same time. At highest temperature of to 450°C, naphtha decreases about 3% but gases increased about 4%. At higher temperature, light hydrocarbon could be cracked more because thermal cracking was faster than catalytic cracking. **Figure 5.2** shows that gas yield increases with higher temperature.

In conclusion, in case of temperature, the temperature of 430°C was the appropriate temperature yielding % oil yield, naphtha, kerosene and gas oil at 69.34, 38.9, 3.85 and 8.74%, respectively.

สถาบันวิทยบริการ
จุฬาลงกรณ์มหาวิทยาลัย

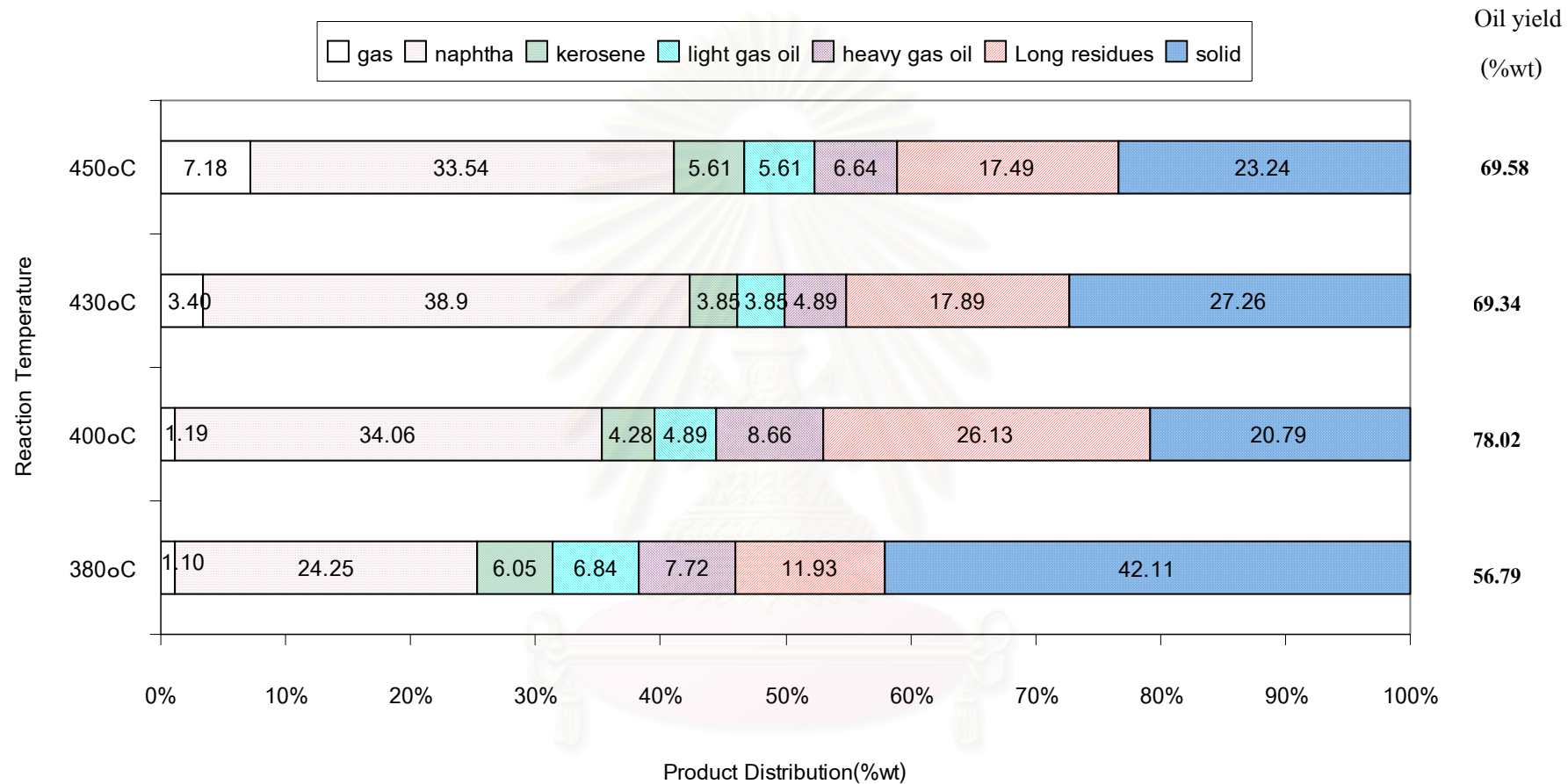


Figure 5.1 SAN conversion on HZSM-5 catalyst with various reaction temperatures.

Reaction condition: 20 g of SAN, 200 psig, 60 min and 2.5 % of catalyst

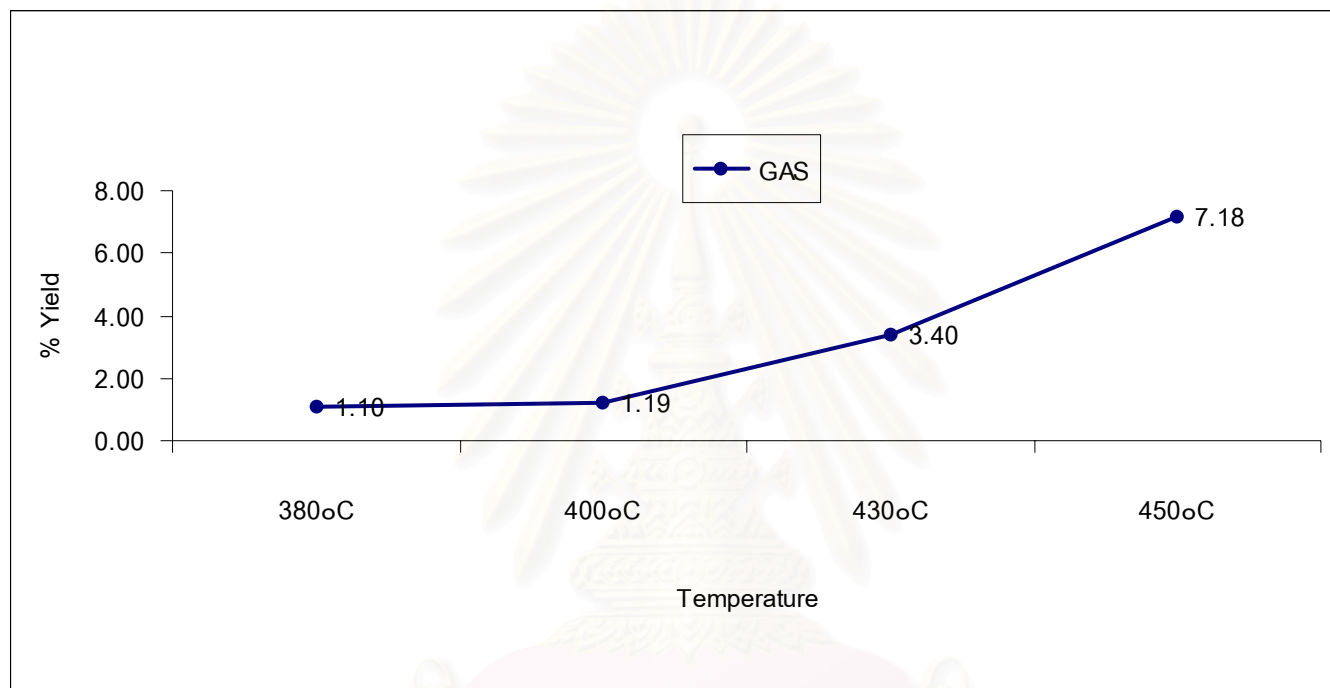


Figure 5.2 Gas yield of SAN on HZSM-5 catalyst with various reaction temperatures.

Reaction condition: 20 g of SAN, 200 psig, 60 min and 2.5% of catalyst

จุฬาลงกรณ์มหาวิทยาลัย

5.2 Influences of amount of catalyst on composition of oil product

The influence of ratio of SAN to catalyst was performed by varying amount of catalyst 0, 0.5, 1.25 and 2.5% by weight. The reaction was carried out at 430 °C, 200 psig of initial hydrogen pressure and 60 min of reaction time. The product yield and composition of products obtained from cracking were shown in **figure 5.3**.

Figure 5.3 shows the comparison of product distribution between amount of catalyst 0, 0.5, 1.25 and 2.5 % by weight. In case of amount of catalyst 0 to 1.25% the percentage of oil yield increases from 62.77 to 75.46%, the percentage of naphtha increases from 27.53 to 45.07% whereas solid decreases from 35.43 to 20.71%. It means that after thermal cracking, the catalytic cracking was better at higher amount of catalyst (1.25%). When the amount of catalyst increases to 2.5% the oil yield largely decreases to 69.34%, and also the percentage of naphtha decreases about 6% whereas solid increase from 20.71 to 27.20%. When using higher amount of catalyst could have higher possibility contraction of catalyst with SAN. As a result it caused rate of coking more than rate of cracking.

In conclusion the ratio of SAN to catalyst parameter is very important for the product selectivity. In this case, the amount of catalyst of 1.25% gave the appropriate % oil yield, naphtha, kerosene and gas oil at 75.46, 45.07, 6.03 and 12.41% respectively.

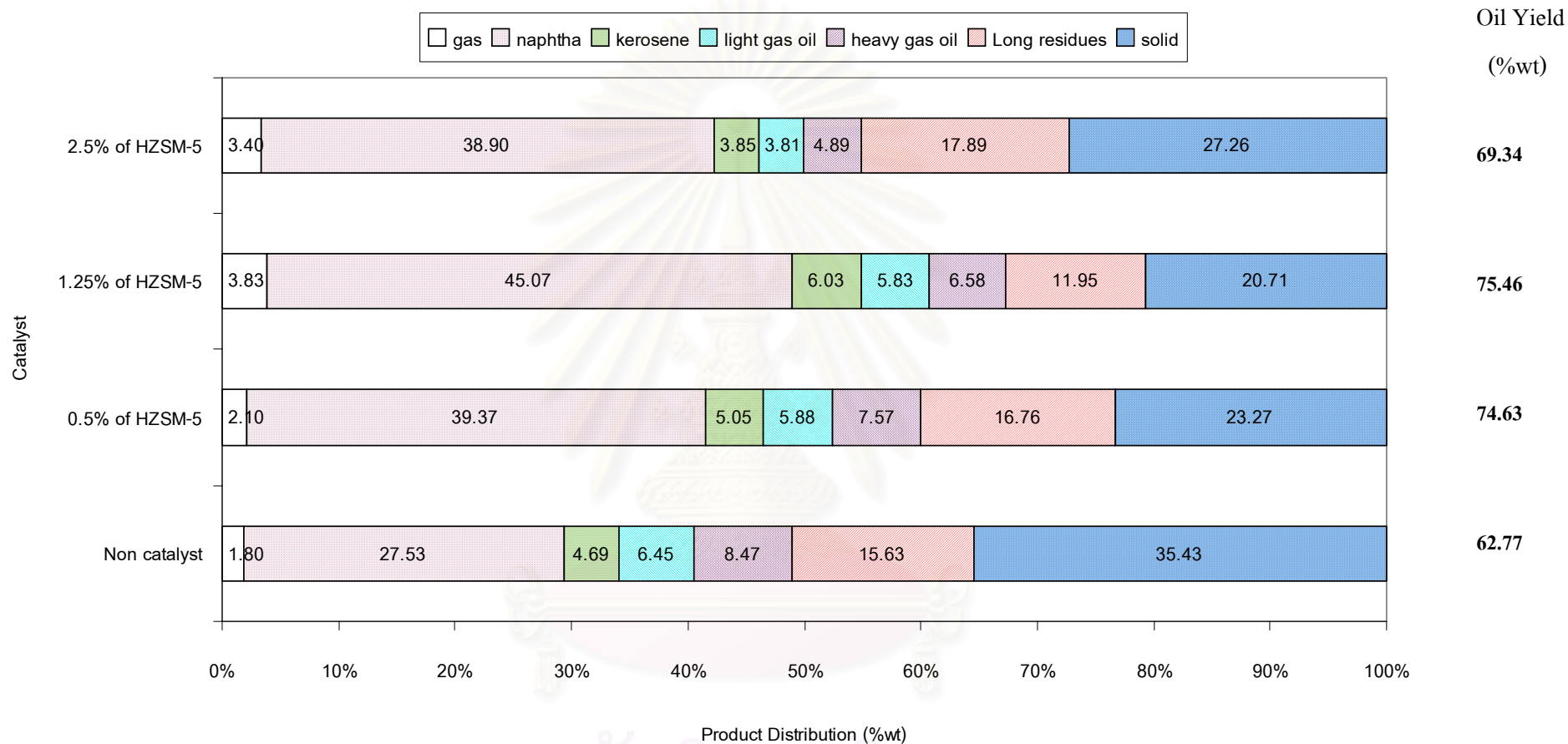


Figure 5.3 SAN conversion on HZSM-5 catalyst with various amounts of catalyst.

Reaction condition: 20 g of SAN, 200 psig, 60 min and 430°C.

5.3 Influences of reaction time on composition of oil product

The Influences of reaction time was performed by various time at 30, 60 and 90 min. SAN was carried out by fixing the condition at 430°C of reaction temperature, 200 psig of hydrogen pressure and amount of catalyst 1.25%. The compositions of products and oil yield from cracking reaction were shown in **figure 5.4**.

Figure 5.4 shows that when the reaction time increased from 30 to 60 min, the % yield of oil increased from 73.16 to 75.46%, naphtha increased from 36.66 to 45.07% except solid yield decreased about 3%. After reaction times over 60 min (90 min), it was observed that the decreasing of % yield of oil and % naphtha, in contrast we noticed the increasing of solid. The solid was increased with time because the more reaction time, the more coke developed at the surface of catalyst. The coke deposits act as a poison, blocking the pore entrance and deactivating the zeolite.

In conclusion, the optimum reaction time was 60 min, because this time gave the highest yield of oil 75.46% and naphtha 45.07 % at condition of 430°C of reaction temperature, 200 psig of hydrogen pressure and amount of catalyst 1.25%.

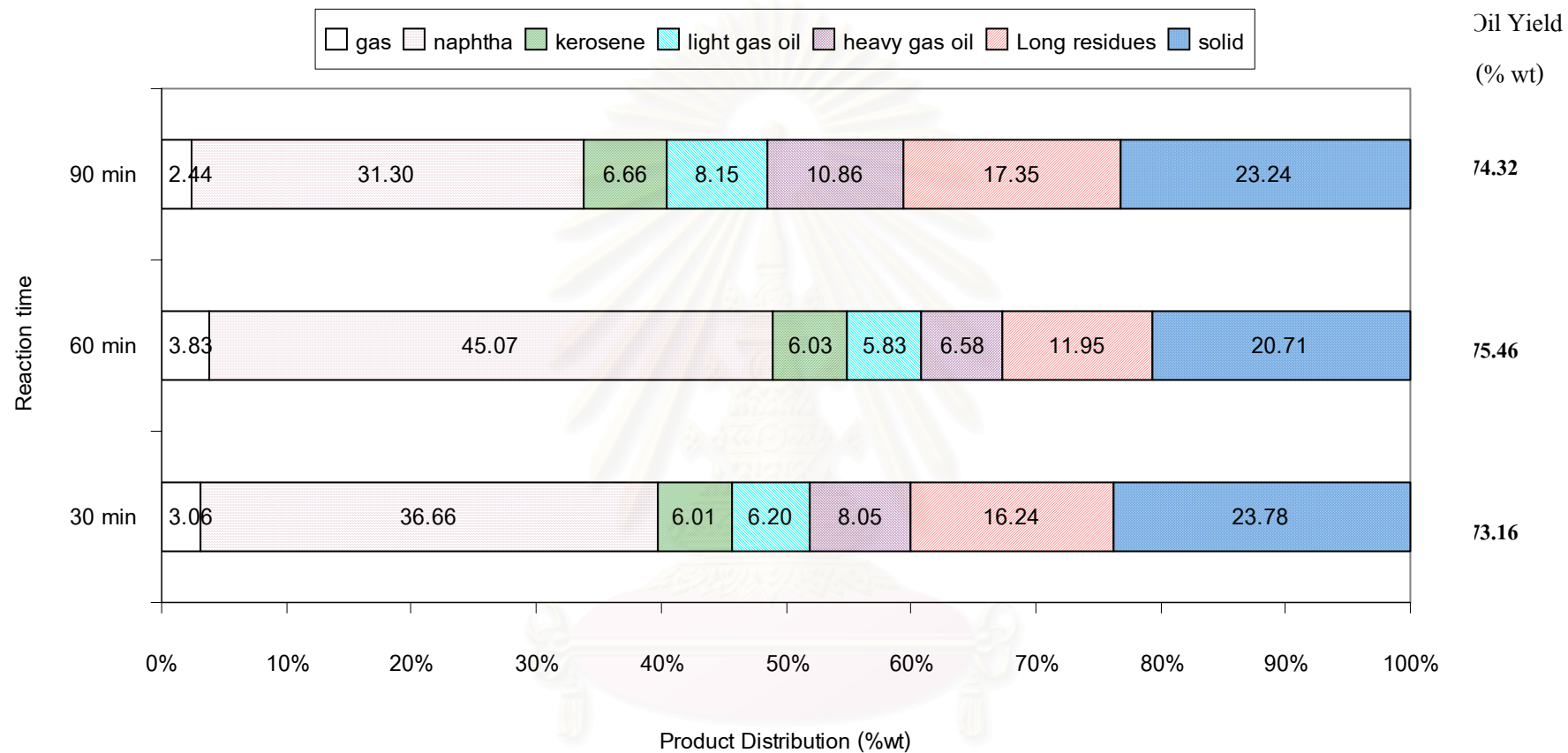


Figure 5.4 SAN conversion on HZSM-5 catalyst with various reaction times.

Reaction condition: 20 g of SAN, 200 psig, 1.25 % of catalyst and 430°C.

5.4 Influences of initial pressure of hydrogen gas on composition of oil product

The influence of hydrogen pressure was performed at various pressures at 0, 100, 200 and 300 psig. Fixing the condition at 430°C of reaction temperature, 60 min of reaction time and amount of catalyst 1.25% carried out SAN. The compositions of products and oil yield from cracking reaction were shown in **figure 5.5**.

Figure 5.5 shows that the product compositions change with change in hydrogen pressure. The increasing of hydrogen pressure from 0-300 psig increased %yield of oil and decreased % solid. In case of hydrogen pressure 0 to 200 psig the percentage of naphtha increased from 28.40 to 45.07% when hydrogen pressure increase to 300 psig the percentage of naphtha more decreased to 36.70%. Normally HZSM-5 gave protons from the structural surface of zeolite to the long chain hydrocarbon for cracking and this hydrogen compensated at the surface by hydrogen feed. These expressed that catalytic cracking occurred less at higher pressure of hydrogen or without hydrogen. It seemed pressure 100 and 200 psig was better than 300 psig and pressure 100, 200 and 300 psig was better than without hydrogen.

In conclusion, in case of initial hydrogen pressure, pressure at 200 psig gave the appropriate % oil yield, naphtha, kerosene and gas oil at 75.46, 45.07, 6.03 and 12.41% respectively.

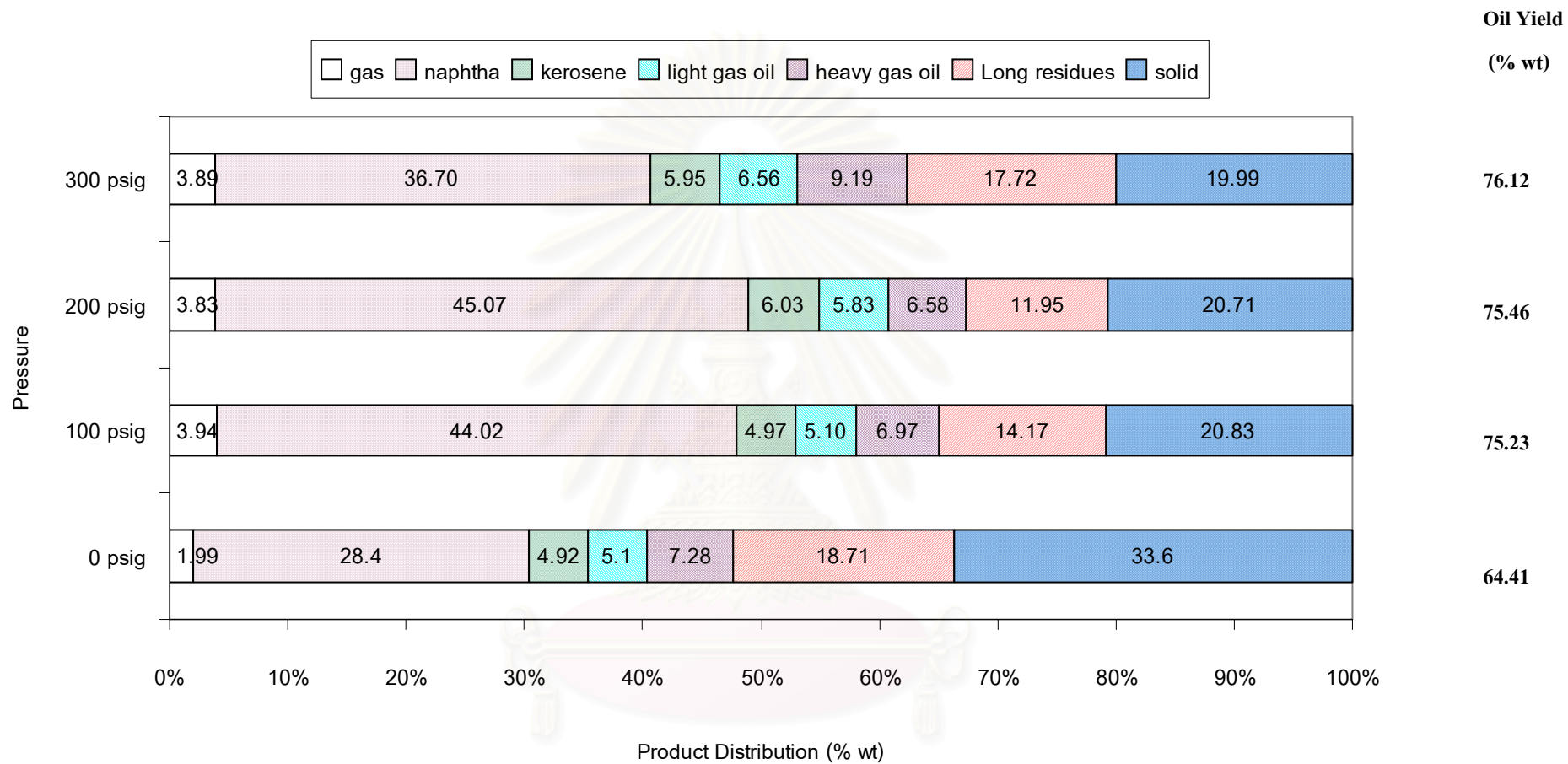


Figure 5.5 SAN conversion on HZSM-5 catalyst with various initial hydrogen pressure.

Reaction condition: 20 g of SAN, 60 min, 1.25% of catalyst and 430°C.

5.5 Characterization of functional groups of oil product by FT-IR

Figure 5.6 shows the functional group compositional analysis of the oil derived from the catalytic cracking reaction of 20 g of SAN, 430 °C of reaction temperature, 200 psig of hydrogen pressure, 1.25% of HZSM-5 catalyst and 60 min of reaction time by Fourier transform infrared (FTIR) spectrometry. The oil product showed a strong presence of both aromatic and aliphatic functional groups. The strong peak at 1600 cm⁻¹ is an indication of the presence of C=C stretching of aromatic skeletal and the additional strong peaks at 1495 cm⁻¹ and 1454 cm⁻¹ also show C=C stretching of aromatic skeletal. However the peak at 1455 cm⁻¹ may overlap with C-H bending of

-CH₂ and -CH₃ functional group. In addition, there are very strong peaks present at 700 and 760 cm⁻¹ and two peaks between 3000 and 3100 cm⁻¹ showing the present of aromatic compounds in the oil. The presence of peaks at 3061 and 3029 cm⁻¹ indicate the presence of C-H stretching of aromatic and the presence of peak at 761 and 700 cm⁻¹ indicates the present of substituted aromatic groups. The low intensity peak at 2225 cm⁻¹ from FTIR spectrum is an indication of presence of -C≡N stretching conjugated with aromatic ring. When SAN is cracked, N from acrylonitrile unit can lead to the formation of ammonia or hydrogen cyanide in the gas fraction and N- containing compounds in the oil fraction.

Figure 5.7 shows the functional group of benzene oil octane number 95 by Fourier transform infrared (FTIR) spectrometry. It showed a strong presence of both aromatic and aliphatic functional groups same the functional groups of oil products. Compared the functional groups of oil product with functional group of benzene oil octane number 95. The aromatic functional group presents show high number.

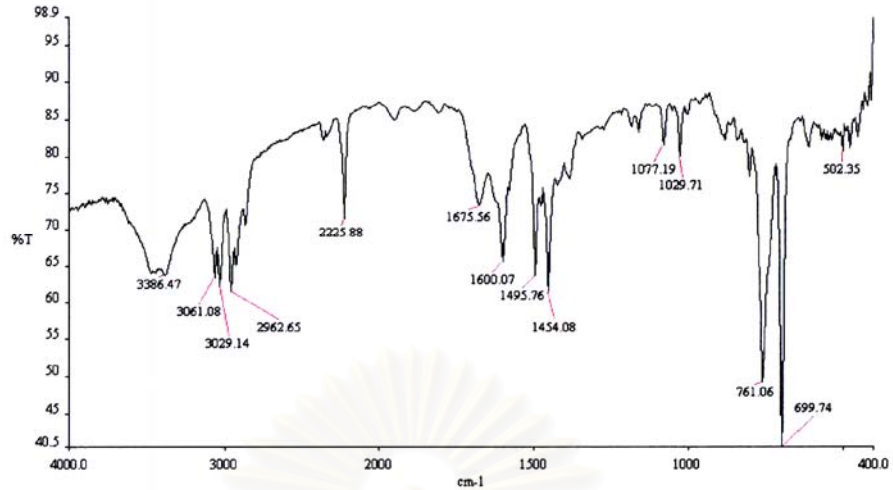


Figure 5.6 FTIR spectrum of oil product derived from catalytic reaction of 20 g of SAN, 430°C of reaction temperature, 200 psig of hydrogen pressure, 60 min of reaction time and 1.25% of catalyst

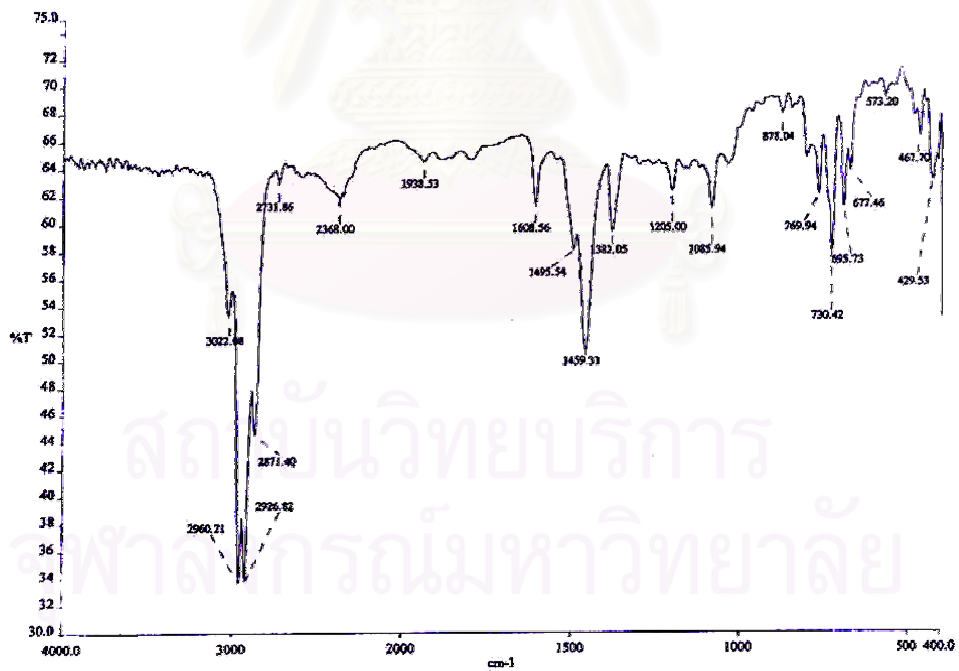


Figure 5.7 FTIR spectrum of benzene oil octane number 95

It is concluded that on the basis of the broad analysis of functional group composition by FTIR that the derived oils from SAN gave spectrum which indicate the aromatic functional group from styrene unit which show high octane number and -CN group from acrylonitrile unit.



สถาบันวิทยบริการ
จุฬาลงกรณ์มหาวิทยาลัย

5.6 Comparison of This Work with Other Works.

The comparison of this work with Kulwadee Pueaknapo [12] was presented with fractions of gases, oil and solids shown in table 5.1.

Table 5.1 Comparison of this work with Kulwadee Pueaknapo

Description	This work	Kulwadee Pueaknapo
Plastic	SAN granule	ABS granule
Catalyst	HZSM-5(0.25g)	Fe/AC(0.6g)
<u>Condition</u>		
Amount of plastic	20g	15g
Temperature	430°C	430°C
Reaction time	60 min	60 min
Atmosphere	H ₂	H ₂
Initial Pressure	15 kg/cm ²	40 kg/cm ²
<u>Results</u>		
Gases (%wt)	3.83	2.6
Oils(%wt)	75.46	67.0
Naphtha(%wt)	45.07	45.0
Kerosene(%wt)	6.03	4.8
Light gas oil(%wt)	5.83	4.5
Heavy gas oil(%wt)	6.58	3.6
Long residues(%wt)	11.95	9.1
Solids(%wt)	20.71	30.4

Kulwadee Pueaknapo studied conversion of acrylonitrile-butadiene-styrene polymer to synthetic fuels on Fe/Activated carbon catalyst. Experiment was done in a microreactor width of 30 mm inside diameter and volume of 70 ml by varying operating conditions. Temperature and pressure of hydrogen gas were first varied between 390 and 450 °C, 20 to 40 kg/cm², respectively. While reaction time, amount of catalyst and percentages loading of iron were varied between 30 and 90 min, 0 and 0.75 g and 1, 5, 10% on activated carbon catalyst, respectively.

From table 5.1 at 430 °C, 60 min, hydrogen pressure 40 kg/cm² and 0.6 g of catalyst Kulwadee Pueaknapo obtained 67.0% of oil yield, naphtha 45%, kerosene 4.8%, light gas oil 4.5%, heavy gas oil 3.6%, long residues 9.1%, 2.6% of gas yield and 30.4% of solid yield. Whereas this work obtained 75.46 % of oil yield, naphtha 45.07%, kerosene 6.03%, light gas oil 5.83%, heavy gas oil 6.58%, and long residues 11.95%, 3.83% of gas yield and 20.71% of solid yield. This result showed higher oil yield than that of Kulwadee Pueaknapo because HZSM-5 used this work was more acidic than Kulwadee's. However the quality of oil yield nearly same %naphtha 40.07 and 45% because thermal cracking having the same rate of reaction. But this work was carried out amount of catalyst lower than that Kulwadee Pueaknapo while used amount of plastic more than.

CHAPTER VI

CONCLUSION AND RECOMMENDATION

The following conclusions from this study have been drawn:

1. The influences of hydrocracking of styrene acrylonitrile copolymer (SAN) by using HZSM-5 catalyst were studied in a microreactor. The temperature was varied from 380-450°C, 0-300 psig of initial hydrogen pressure, 30-90 min of reaction time and amounts of catalyst 0-2.5% by weight. Using GC Simulate Distillation and Fourier-Transform Infrared Spectrometer performed analysis of the products.

2. From the experimental results obtained from this study, it may be concluded as follow:
 - 2.1 Suitable reaction temperature is 430°C because the characteristic of obtained product is true oil and contains the highest quantity of naphtha and other oil component.
 - 2.2 Suitable catalytic is 1.25% by weight because the higher amount of catalyst, the higher possibility to contact the polymer. But too high amount of catalyst (2.5% by weight) caused higher rates of cracking as same as coking.
 - 2.3 Suitable reaction time is 60 min because it is obtained the maximum percentages of yield and naphtha and lowest percentages of solid. The longer reaction time (90 min) caused coking at surface of catalyst, therefore it shows the decreasing of naphtha and yield.

2.4 Suitable hydrogen pressure is 200 psig was the appropriate condition because gave the highest naphtha 45.07%.

At temperature 430⁰C, amount of catalyst 1.25% by weight, reaction time 60 min and hydrogen pressure 200 psig, the oil yield, gas, naphtha, kerosene, gas oil, long residues and solid were 75.46, 3.83, 45.07, 6.03, 12.41, 11.95, 20.71%, respectively.

3. The derived oils show aromatic functional group by means of Fourier-Transform Infrared Spectrometer, which indicated the presence of high octane number and also show low intensity of N-containing in oil.

Recommendation:

The recommendation for further study of this thesis to study mole ratio Si/Al of HZSM-5 catalyst and investigate the change of local structure of Al in ZSM-5 framework during the modification of cation form such as Ga, Ti Fe and Zn respectively.

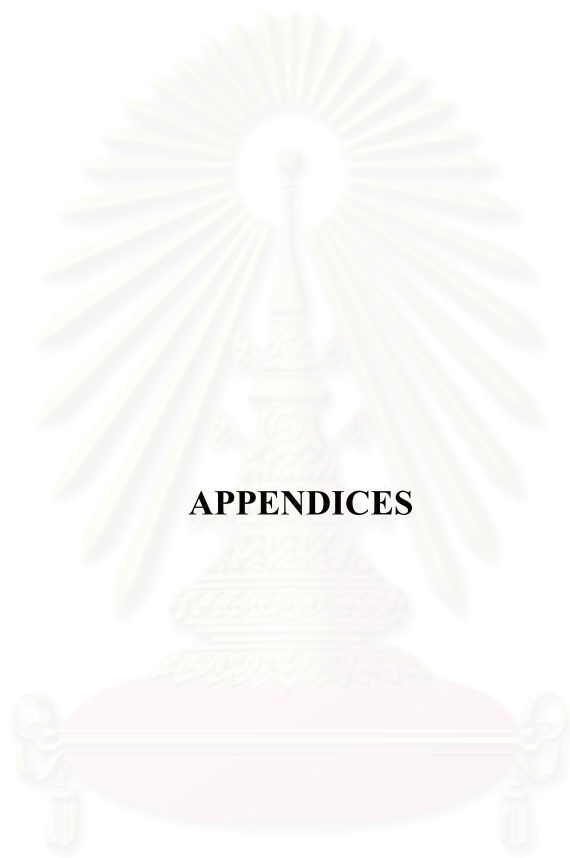
สถาบันวิทยบริการ
จุฬาลงกรณ์มหาวิทยาลัย

REFERENCES

1. Suzuki, T.; Shiro, T.; Kanno, T.; Aratani, K.; Katsura.; and Ikenaga, N. Promoting Effect of Sulfur Compounds on the Degradation of Polyethylene. Energy & Fuels .16(2002): 1314-1320.
2. Luo, M.; and Curtis, C. W. Thermal and catalytic coprocessing of Illinois No.6 with model and commingled waste plastics. Fuel Processing Technology. 49 (1996): 91-117.
3. Polymer Terminology: Styrene-Acrylonitrile Copolymer (SAN)[Online]. Available from: http://www.Polymerdoctor.com/fine/plsql/dictionary_main_new?category_idm=8658[2003, November 11]
4. Poly(styrene-co-acrylonitrile) information and properties[Online]. Available from: <http://www.Polymerprocessing.com/polymers/SAN.html> [2003, November 17]
5. Ghosh, P. Polymer science and technology plastics, Rubbers, Blends and Composites. Teta McGraw-Hill Publishing Company Limited 1990.
6. Overview-Styrene Acrylonitrile (SAN), Modeled [Online]. Available from: <http://www.matweb.com/search/Specific Material ext. asp?bassnum=04920> [2003, November 17]
7. Feng, Z.; Zhao, J.; Rockwell, J.; Bailey, D., Huffman, G., "Direct Liquefaction of Waste Plastics and Coliquefaction of Coal-plastic Mixtures", Fuel Processing Technology. 49(1996): 17-30
8. Agado, J.; Sotelo, J. L.; Serrano, D. P.; Calles, J. A.; Escola, J. M. "Catalytic Conversion of Polyolefins into Liquid Fuels over MCM-41: Comparison with HZSM-5 and Amorphous SiO₂- Al₂O₃." Energy Fuels. 11(1997): 1225-1232
9. Uemichi, Y.; Nakamura, J.; Itoh, T.; Sugioka, M. "Conversion of Polyethylene into Gasoline-Rang Fuels by Two-Stage Catalytic Degradation Using Silica-Alumina and HZSM-5 Zeolite." Ind. Eng. Chem. Res. 38 (1999): 385-390

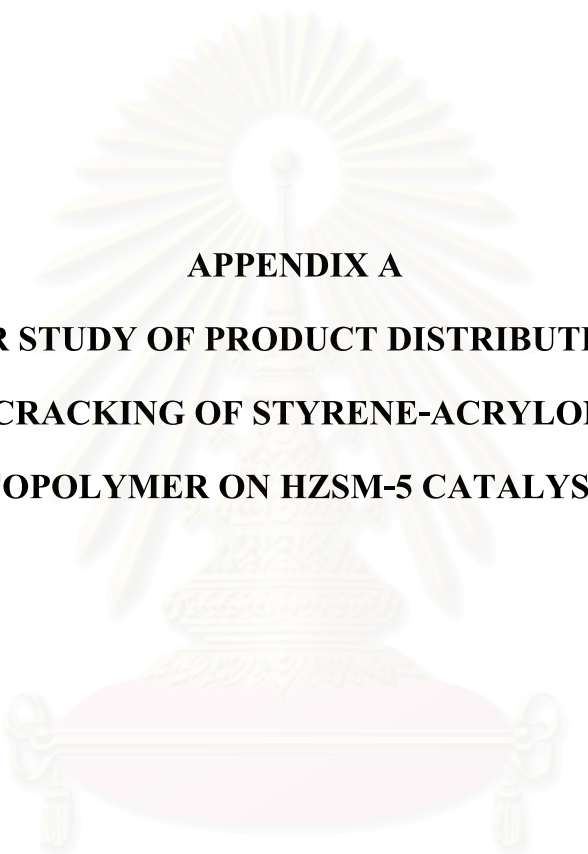
10. Brebu, M.; Uddin, A.; Muto, A.; Sakata, Y. "Composition of Nitrogen-Containing Compounds in Oil Obtained from Acrylonitril-Butadiene-Styrene Thermal Degradation", Energy Fuels. 14 (2000): 920-928
11. Somsuk Trisupakiti. Conversion of Polyethylene into Gasoline on HZSM-5 Catalyst. Master's Thesis, Program of Petrochemistry and Polymer Science, Faculty of Science, Chulalongkorn University, 2000.
12. Kulwadee Peaknapo. Conversion of Acrylonitrile-Butadiene-Styrene Polymer to Synthetic Fuels on Fe/Activated Carbon Catalyst. Master's Thesis, Program of Petrochemistry and Polymer Science, Faculty of Science, Chulalongkorn University, 2001.
13. Brebu, M.; Uddin, A.; Muto, A.; Sakata, Y. "Catalytic Degradation of Acrylonitrile-Butadiene-Styrene into Fuel Oil 1. The Effect of Iron Oxides on the Distribution of Nitrogen-Containing Compounds", Energy Fuels .15(2001): 559-564
14. Seo Y., Lee K., Shin D., "Investigation of catalytic degradation of high-density polyethylene by hydrocarbon group type analysis." J. Anal. Appl. Pyrolysis. 00 (2002):1-16
15. Alan E. Eelson and the University of Alberta. 2002. Catalysis by Zeolites.[Online]. Available from: <http://www.ualberta.ca/~oane/son/Tutorials/catalysis-zeolites.html>[2004, February 25]
16. Szostak, R. Molecular Sieve Principle of Synthesis and Identification. New York: Norstand Reinhold, 1989.
17. The University of Manchester. 1998. Modelling of Zeolite Catalysis.[Online]. Available from: <http://mch3w.ch.man.ac.uk/theory/posters/emw/poster.htm> [2004, February 25]

18. Bruce, D.G., and James, R,k. Chemistry of catalytic Processes. New York: McGraw-Hill Book company, 1979.
19. Dwyer, A. An Introduction to Zeolite Molecular sieves. Chichester: John Wiley and Sons, 1988.
20. Chockchai Jewrasumneay. Deactivation of HZSM-5 types catalyst by catalyst by carbonaceous compounds for methanol conversion. Chemical Engineering, Master's thesis Chulalongkorn University, 1991.
21. ปราโมทย์ ไชยเวช. ปิโตรเลียมเทคโนโลยี. กรุงเทพมหานคร: ภาควิชาเคมีเทคนิค, คณะวิทยาศาสตร์ จุฬาลงกรณ์มหาวิทยาลัย, 2537.
22. Tiong, S. S Ind. Eng. Chem. Res. 31(1992): 1881-1889.
23. นงเยาว์ ชูติวณิชกุล. อิทธิพลของทัลค์และไมกาที่มีต่อสมบัติของพอลิพรอพิลีน. วิทยานิพนธ์ ปริญญาโท สาขาวิศวกรรมเคมี คณะวิศวกรรมศาสตร์ จุฬาลงกรณ์ มหาวิทยาลัย, 2543.



APPENDICES

สถาบันวิทยบริการ
จุฬาลงกรณ์มหาวิทยาลัย



APPENDIX A
DATA FOR STUDY OF PRODUCT DISTRIBUTION FROM
HYDROCRACKING OF STYRENE-ACRYLONITRILE
COPOLYMER ON HZSM-5 CATALYST

สถาบันวิทยบริการ
จุฬาลงกรณ์มหาวิทยาลัย

Table A-1 Data for study of product distribution from hydrocracking of styrene acrylonitrile copolymer on HZSM-5 catalysis

Batch No	Condition				SAN (g)	Cat (g)	Gas		Solid		Oil Yield(%)
	Temp(⁰ C)	P (psig)	Time (min)	Cat (g)			Amount(g)	Yield(%)	Amount(g)	Yield(%)	
1	350	100	30	0.10	20.03	0.12	0.18	0.90			Oil+Solid
2	350	200	30	0.10	20.03	0.11	0.17	0.85			Oil+Solid
3	350	100	60	0.10	20.03	0.10	0.18	0.90			Oil+Solid
4	350	200	60	0.10	20.04	0.10	0.33	1.65			Oil+Solid
5	350	100	30	0.50	20.03	0.51	0.24	1.20			Oil+Solid
6	350	200	30	0.50	20.05	0.51	0.17	0.85			Oil+Solid
7	350	100	60	0.50	20.02	0.51	0.17	0.85			Oil+Solid
8	350	200	60	0.50	20.00	0.50	0.19	0.95			Oil+Solid
9	380	100	30	0.10	20.04	0.10	0.14	0.20			Oil+Solid
10	380	200	30	0.10	20.02	0.10	0.24	1.20			Oil+Solid
11	380	100	60	0.10	20.00	0.10	0.14	0.70	8.96	44.80	54.50
12	380	200	60	0.10	20.06	0.10	0.18	0.90	9.13	45.51	53.59

Table A-1 (continue)

13	380	100	30	0.50	20.06	0.50	0.13	0.65			Oil+Solid
14	380	200	30	0.50	20.02	0.50	0.15	0.75			Oil+Solid
15	380	100	60	0.50	20.07	0.51	0.19	0.95	8.86	44.15	54.90
16	380	200	60	0.50	20.04	0.51	0.22	1.1	8.44	42.11	56.79
17	380	200	60	0.00	20.04	0.00	0.22	1.10	9.18	45.81	53.09
18	350	100	30	0.00	20.05	0.00	0.12	0.60			Oil+Solid
19	380	0	60	0.50	20.02	0.50	0.14	0.70	11.70	58.44	40.86
20	400	200	60	0.50	20.05	0.50	0.24	0.12	4.17	20.79	78.02
21	430	200	60	0.50	20.03	0.50	0.68	3.40	5.46	27.26	69.34
22	450	200	60	0.50	20.05	0.50	1.44	7.18	4.66	23.24	69.58
23	430	200	60	0.25	20.06	0.25	0.77	3.83	4.15	20.71	75.46
24	430	200	60	0.10	20.00	0.10	0.42	2.10	4.65	23.27	74.63
25	430	200	60	0.00	20.01	0.00	0.36	1.80	7.09	35.43	62.77

Table A-1 (continue)

26	430	100	60	0.25	0.25	0.25	0.79	3.94	4.17	20.83	75.23
27	430	200	30	0.25	20.02	0.25	0.61	3.05	4.76	23.78	73.16
28	430	200	90	0.25	20.01	0.25	0.49	2.44	4.65	23.24	74.32
29	430	300	60	0.25	20.06	0.25	0.78	3.89	4.01	19.99	76.12
30	430	0	60	0.25	20.03	0.25	0.40	1.99	6.73	33.60	64.41

สถาบันวิทยบริการ
จุฬาลงกรณ์มหาวิทยาลัย

Table A-2: The percentage of oil composition by GC Simulated Distillation.					
BATCH NO	Naphtha 65-200 ^o C	Kerosene 200-250 ^o C	Light Gas Oil 300-350 ^o C	Heavy Gas Oil 300-350 ^o C	Long Residues >350 ^o C
11	28.59	9.56	12.95	16.58	32.32
12	32.42	11.63	13.28	15.80	26.26
15	35.97	11.20	12.80	14.73	25.30
16	42.71	10.65	12.04	13.60	21.00
17	29.21	9.82	12.39	16.50	30.08
19	31.52	6.95	10.58	14.77	34.28
20	43.65	5.49	6.27	11.11	33.49
21	56.10	5.55	5.50	7.05	25.80
22	48.20	8.06	9.06	9.54	25.14
23	59.73	7.99	7.72	8.72	15.84
24	52.75	6.77	7.88	10.14	22.46
25	34.86	7.47	10.27	13.50	24.90
26	58.52	6.60	6.78	9.26	18.84
27	50.11	8.21	8.47	11.01	22.20
28	42.12	8.96	10.96	14.61	23.35
29	48.21	7.82	8.62	12.07	23.28
30	44.09	7.64	7.92	11.31	29.04

APPENDIX B

GRAPH OF PRODUCT FROM GAS CHROMATOGRAPH

(GC Simulated Distillation)

- Figure B.1 Oil composition at condition 380 °C of reaction temperature, 200 psig of hydrogen, 60 min of reaction time and 2.5% of HZSM-5 catalyst by GC Simulated Distillation.
- Figure B.2 Oil composition at condition 400 °C of reaction temperature, 200 psig of hydrogen, 60 min of reaction time and 2.5% of HZSM-5 catalyst by GC Simulated Distillation.
- Figure B.3 Oil composition at condition 430 °C of reaction temperature, 200 psig of hydrogen, 60 min of reaction time and 2.5% of HZSM-5 catalyst by GC Simulated Distillation.
- Figure B.4 Oil composition at condition 450 °C of reaction temperature, 200 psig of hydrogen, 60 min of reaction time and 2.5% of HZSM-5 catalyst by GC Simulated Distillation.
- Figure B.5 Oil composition at condition 0.5% of HZSM-5 catalyst, 430 °C of reaction temperature, 200 psig of hydrogen and 60 min of reaction time by GC Simulated Distillation.
- Figure B.6 Oil composition at condition 1.25% of HZSM-5 catalyst, 430 °C of reaction temperature, 200 psig of hydrogen and 60 min of reaction time by GC Simulated Distillation.

- Figure B.7 Oil composition at condition 30 min of reaction time, 430 °C of reaction temperature, 1.25% of HZSM-5 catalyst and 200 psig of hydrogen by GC Simulated Distillation.
- Figure B.8 Oil composition at condition 90 min of reaction time, 430 °C of reaction temperature 1.25% of HZSM-5 catalyst, 200 psig of hydrogen and by GC Simulated Distillation.
- Figure B.9 Oil composition at condition 100 psig of hydrogen, 430 °C of reaction temperature, 1.25% of HZSM-5 catalyst and 60 min of reaction time by GC Simulated Distillation.
- Figure B.10 Oil composition at condition 300 psig of hydrogen, 430 °C of reaction temperature, 1.25% of HZSM-5 catalyst and 60 min of reaction time by GC Simulated Distillation.
- Figure B.11 Oil composition at condition 200 psig of hydrogen, 430 °C of reaction temperature, non-catalyst and 60 min of reaction time by GC Simulated Distillation.
- Figure B.12 Oil composition at condition 430 °C of reaction temperature, 1.25% of HZSM-5 catalyst, non-hydrogen and 60 min of reaction time by GC Simulated Distillation.

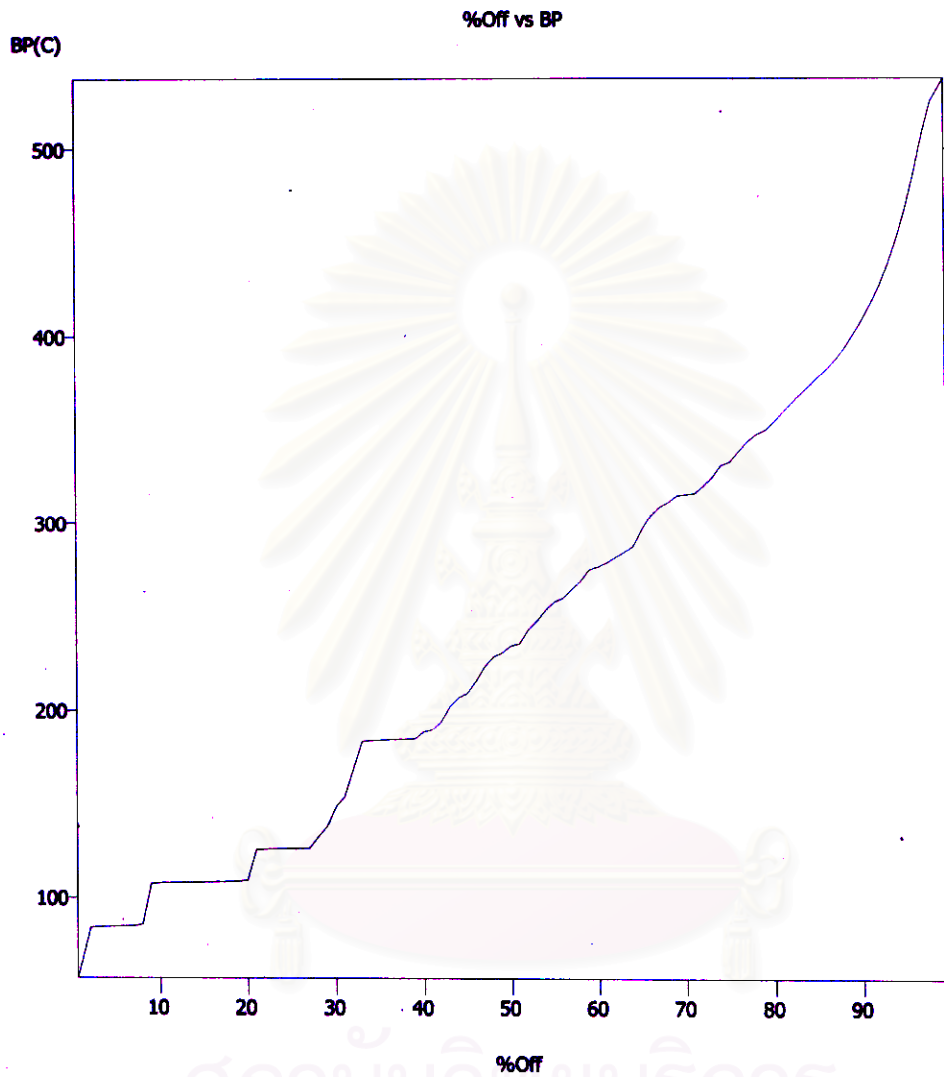


Figure B.1 Oil composition at condition 380 °C of reaction temperature, 200 psig of hydrogen, 60 min of reaction time and 2.5% of HZSM-5 catalyst by GC Simulated Distillation.

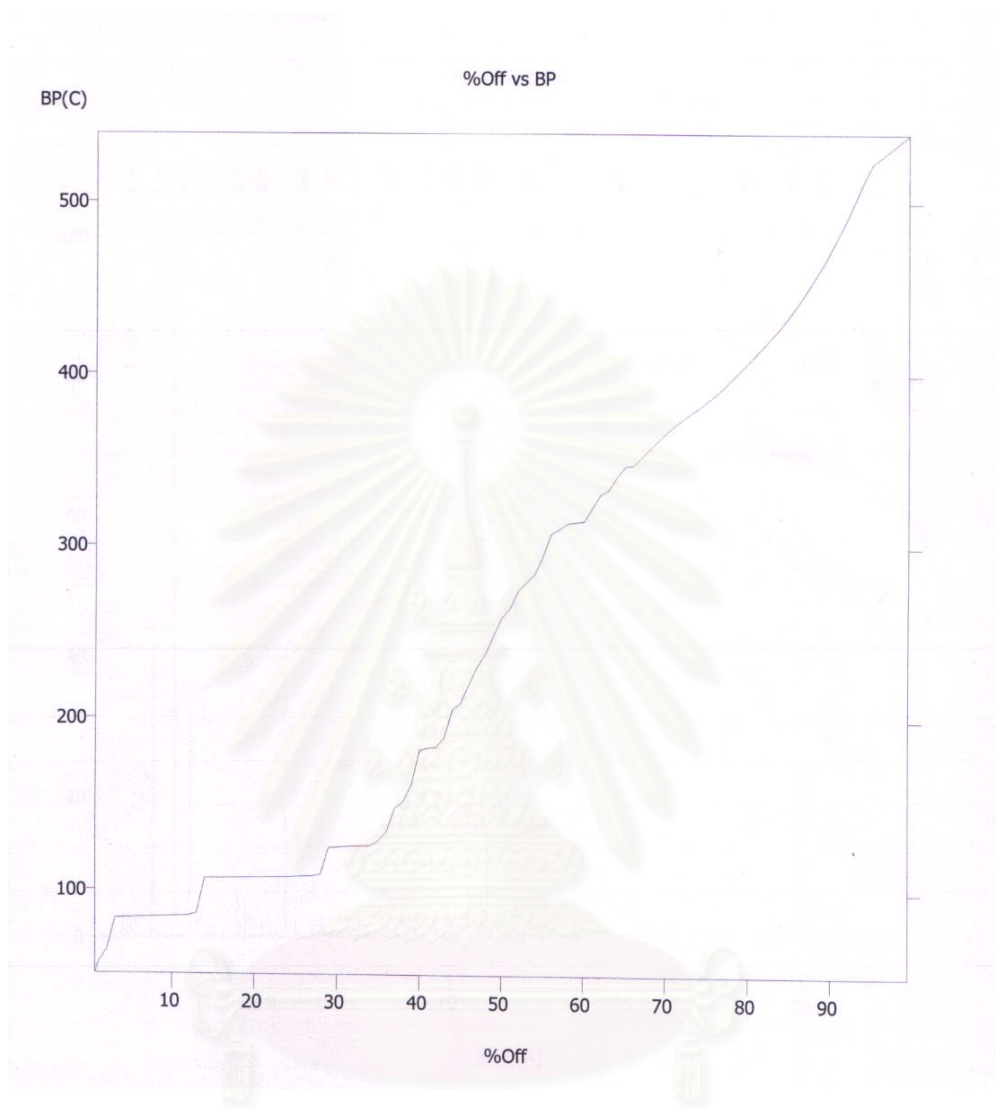


Figure B.2 Oil composition at condition 400 °C of reaction temperature, 200 psig of hydrogen, 60 min of reaction time and 2.5% of HZSM-5 catalyst by GC Simulated Distillation.

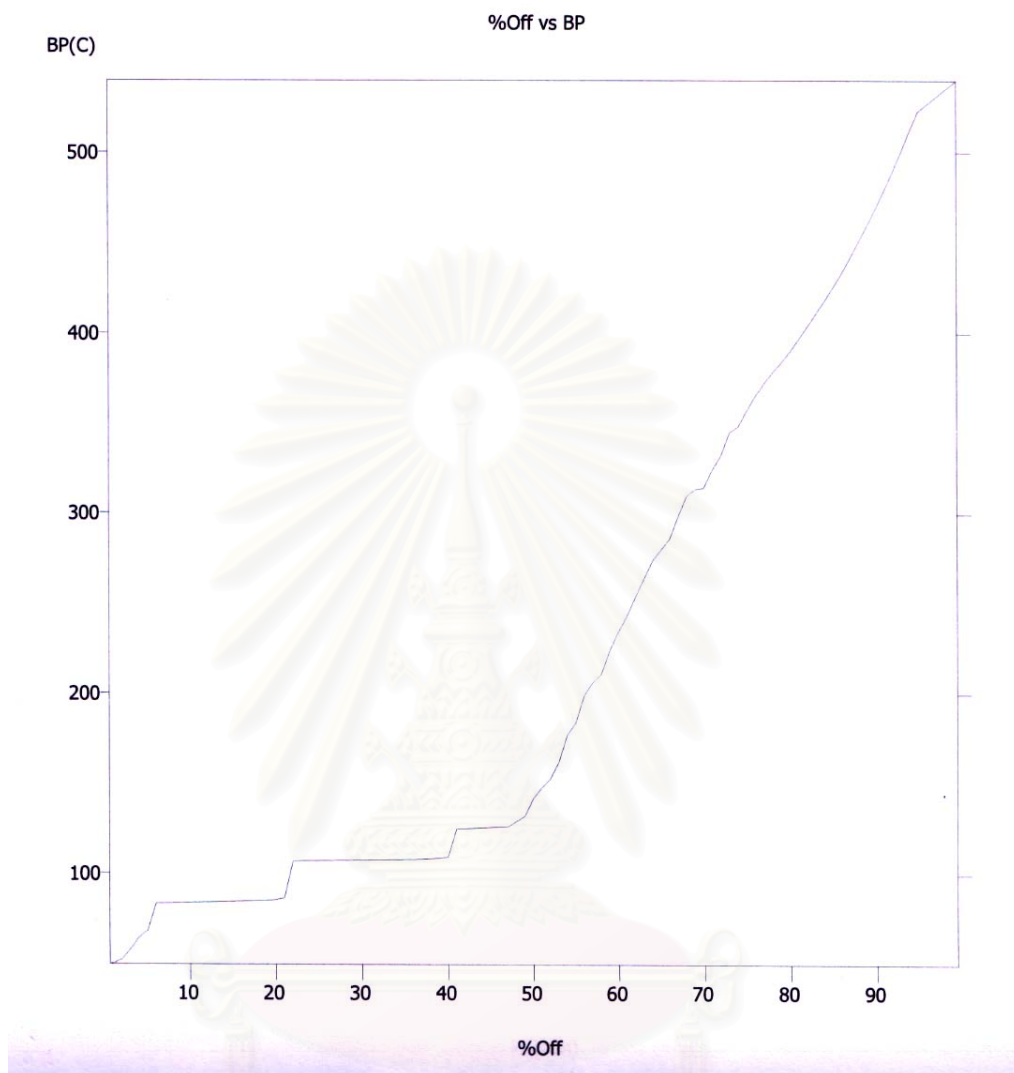
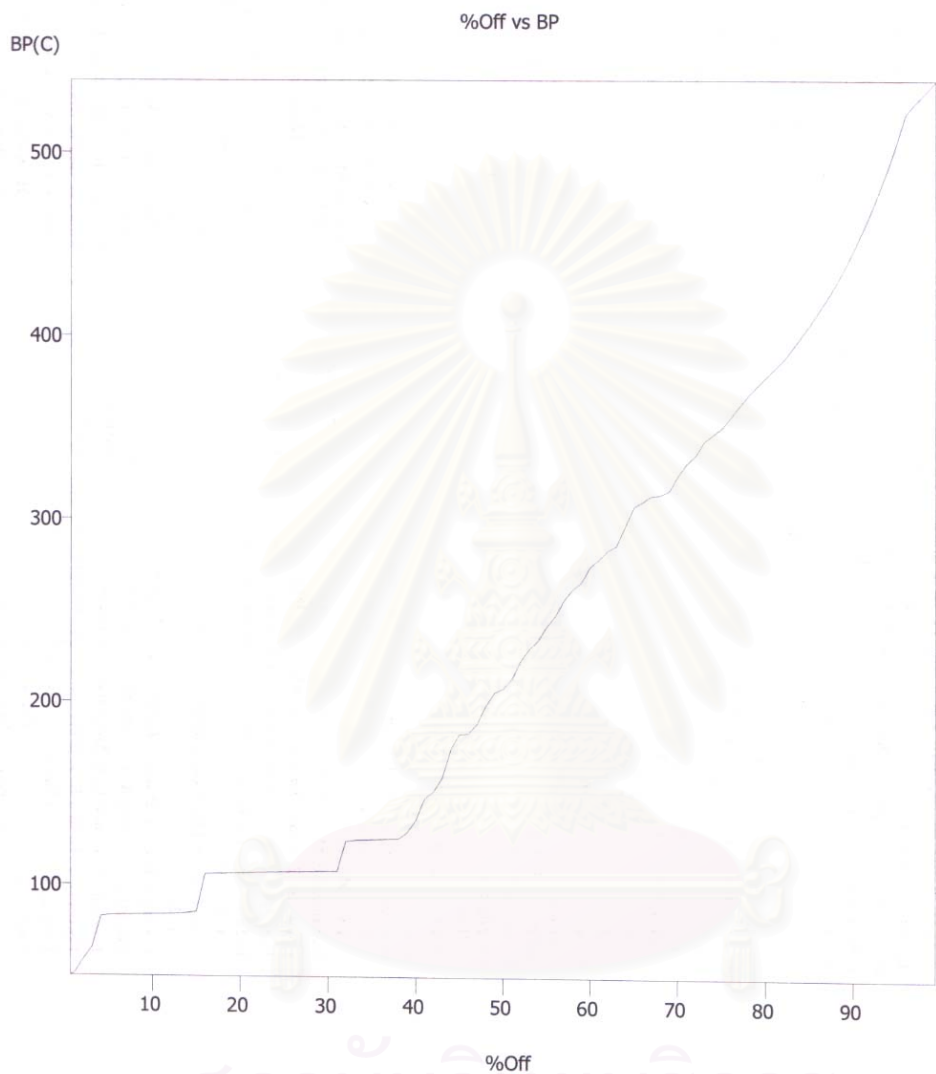


Figure B.3 Oil composition at condition 430 °C of reaction temperature, 200 psig of hydrogen, 60 min of reaction time and 2.5% of HZSM-5 catalyst by GC Simulated Distillation.



สถาบันวิทยบริการ
จุฬาลงกรณ์มหาวิทยาลัย

Figure B.4 Oil composition at condition 450 °C of reaction temperature, 200 psig of hydrogen, 60 min of reaction time and 2.5% of HZSM-5 catalyst by GC Simulated Distillation.

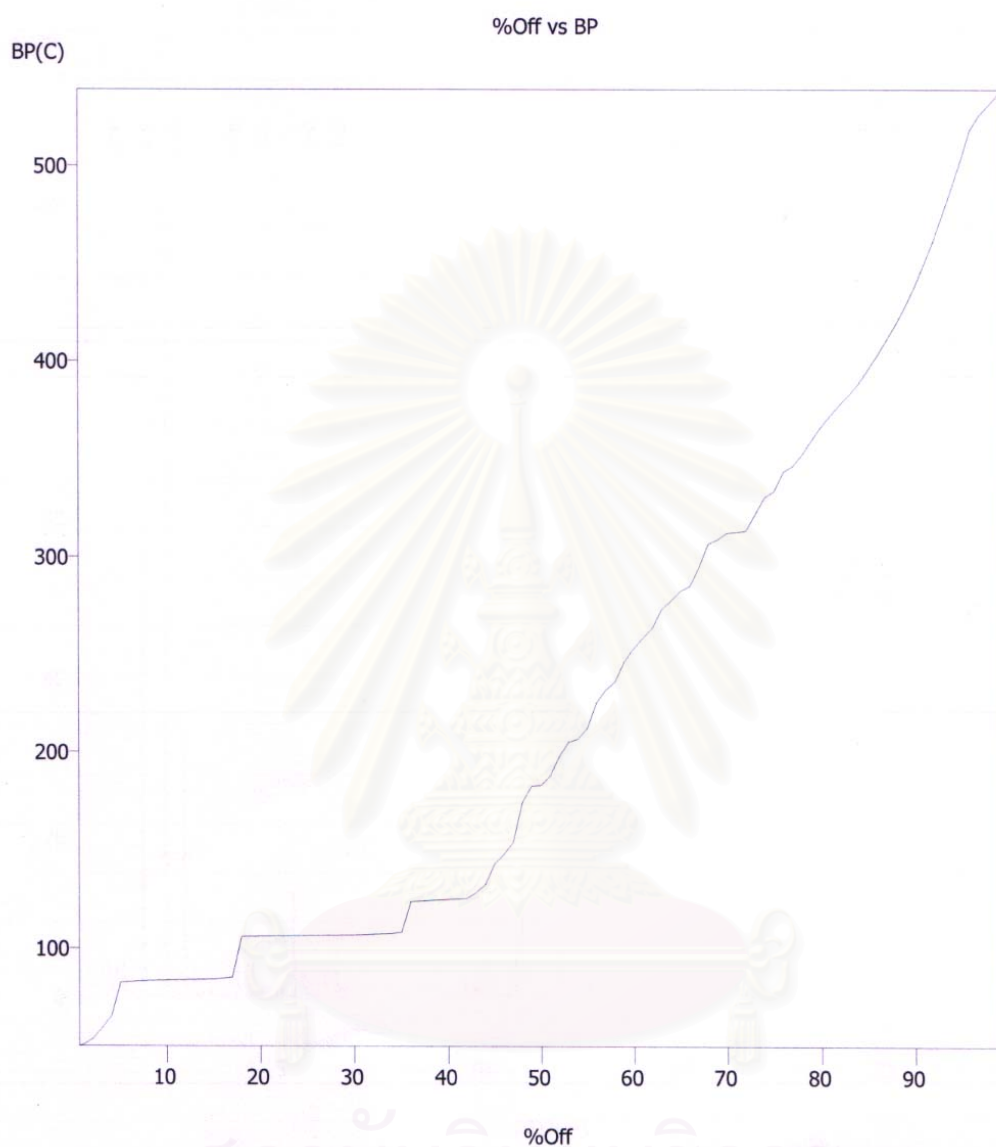


Figure B.5 Oil composition at condition 0.5% of HZSM-5 catalyst, 430 °C of reaction temperature, 200 psig of hydrogen and 60 min of reaction time by GC Simulated Distillation.

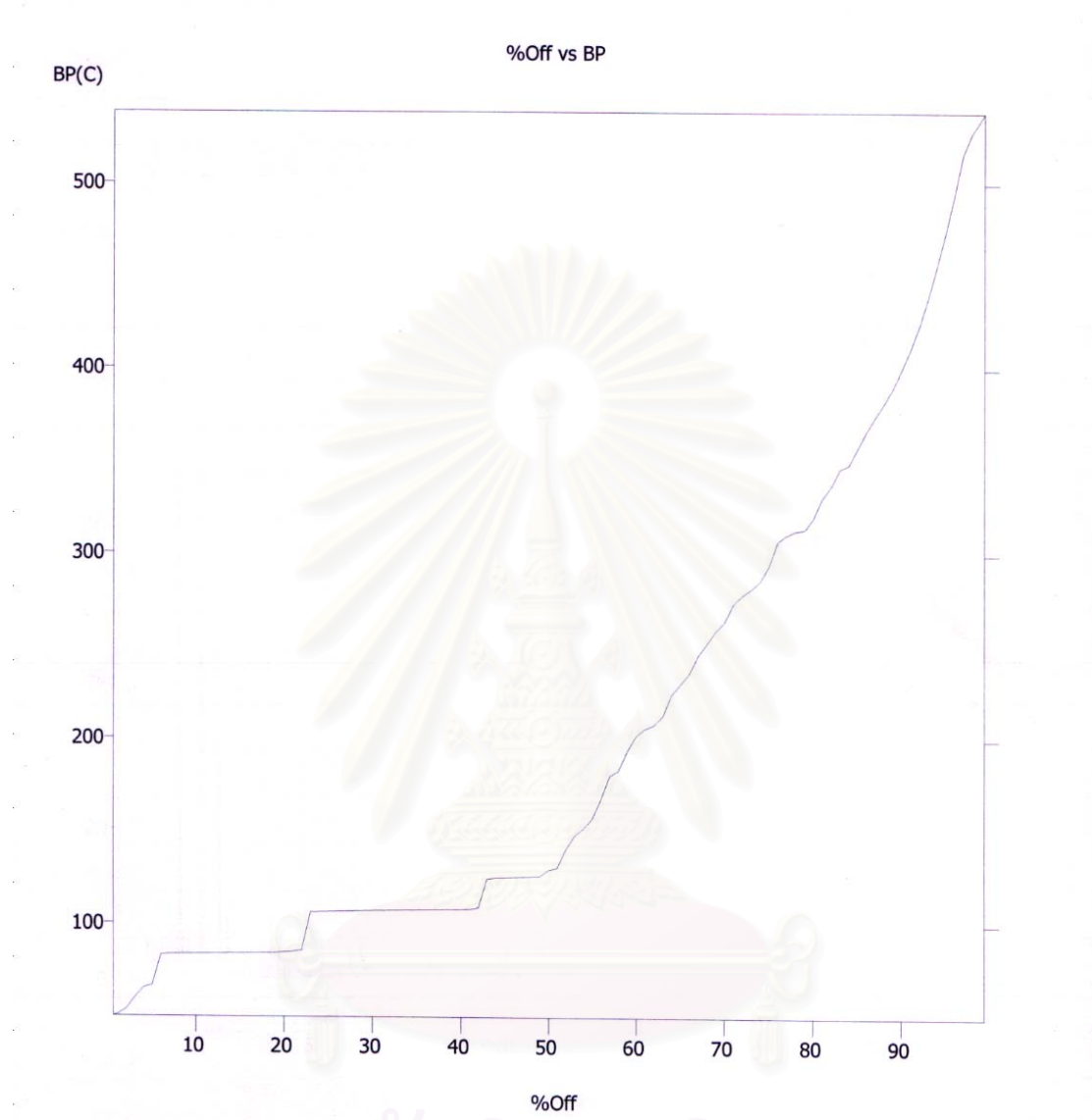


Figure B.6 Oil composition at condition 1.25% of HZSM-5 catalyst, 430 °C of reaction temperature, 200 psig of hydrogen and 60 min of reaction time by GC Simulated Distillation.

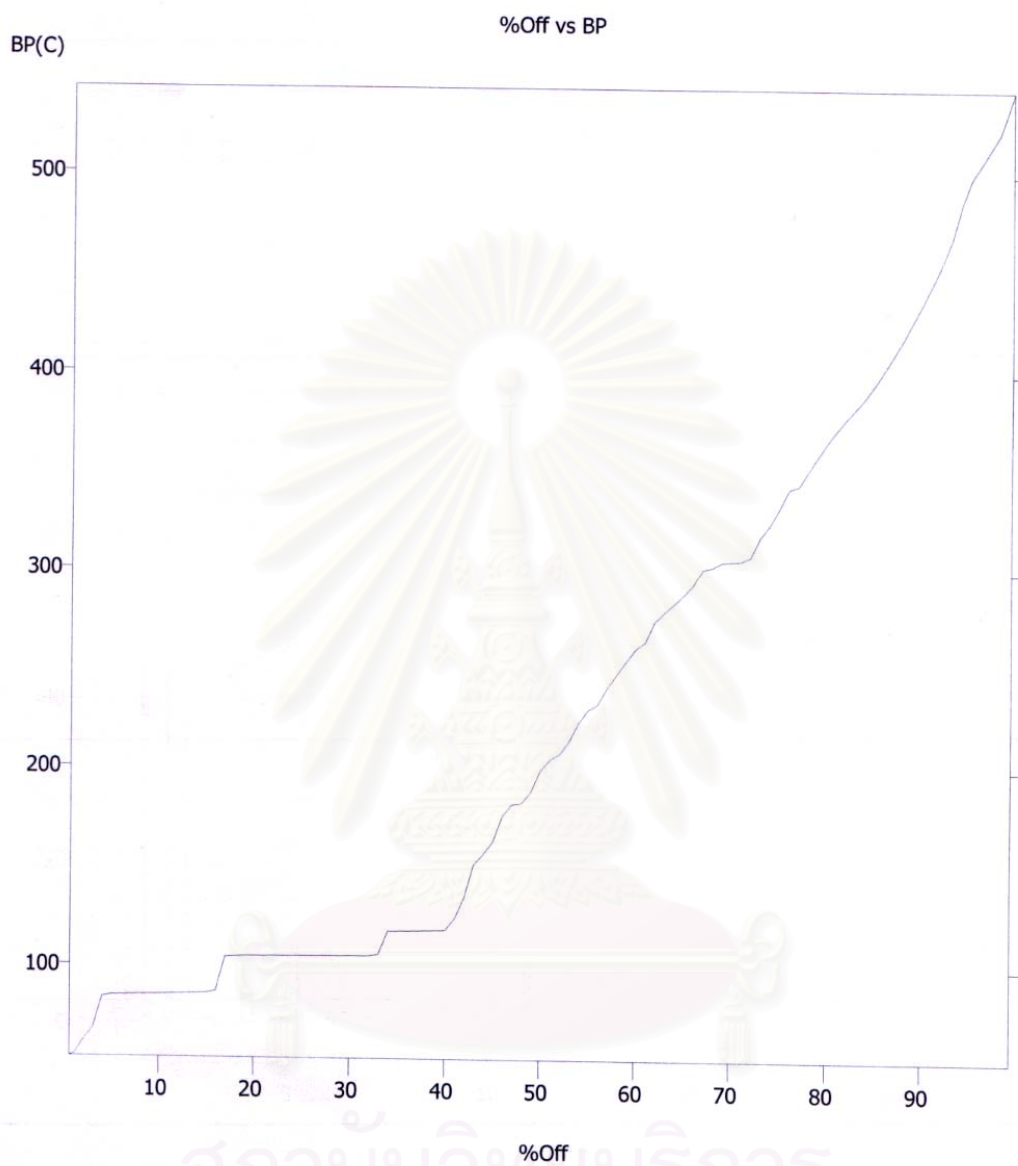


Figure B.7 Oil composition at condition 30 min of reaction time, 430 °C of reaction temperature, 1.25% of HZSM-5 catalyst and 200 psig of hydrogen by GC Simulated Distillation.

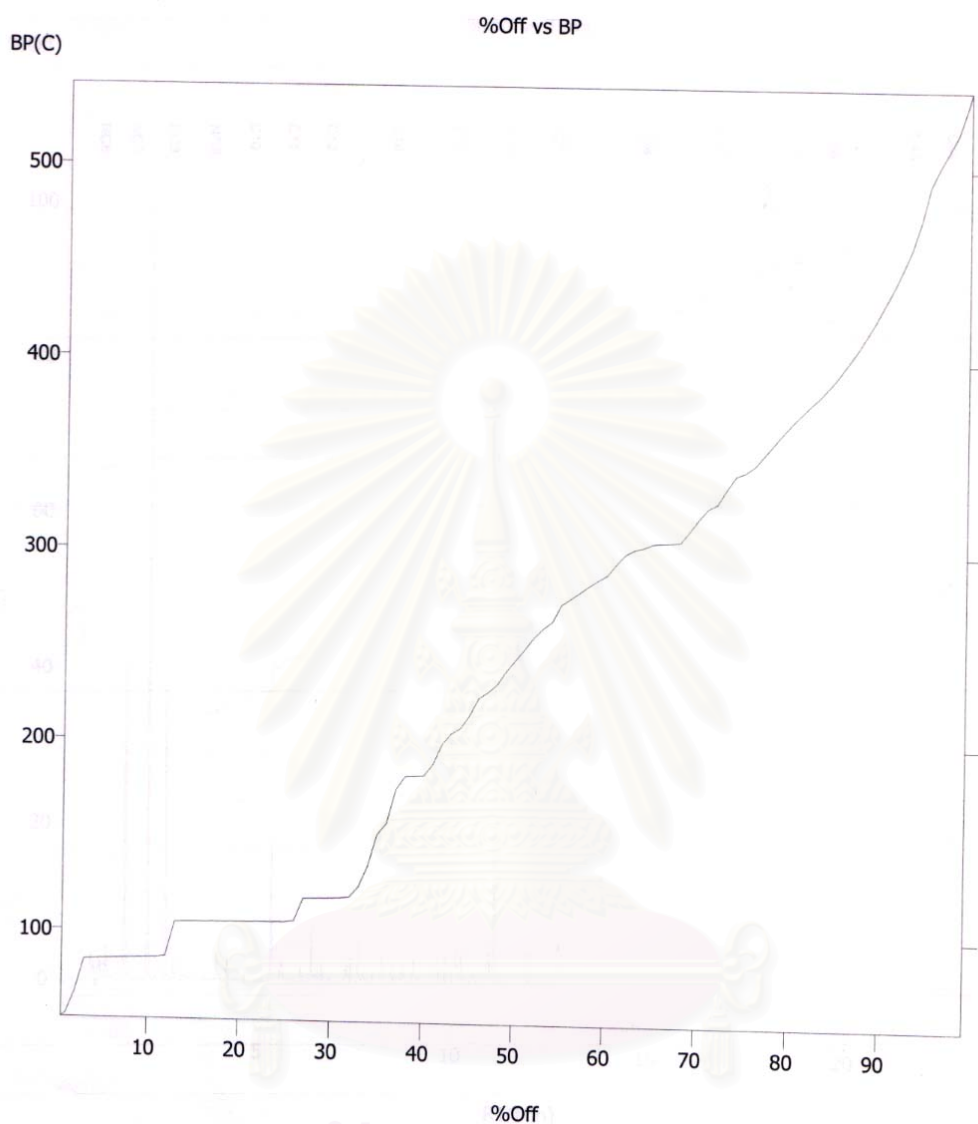
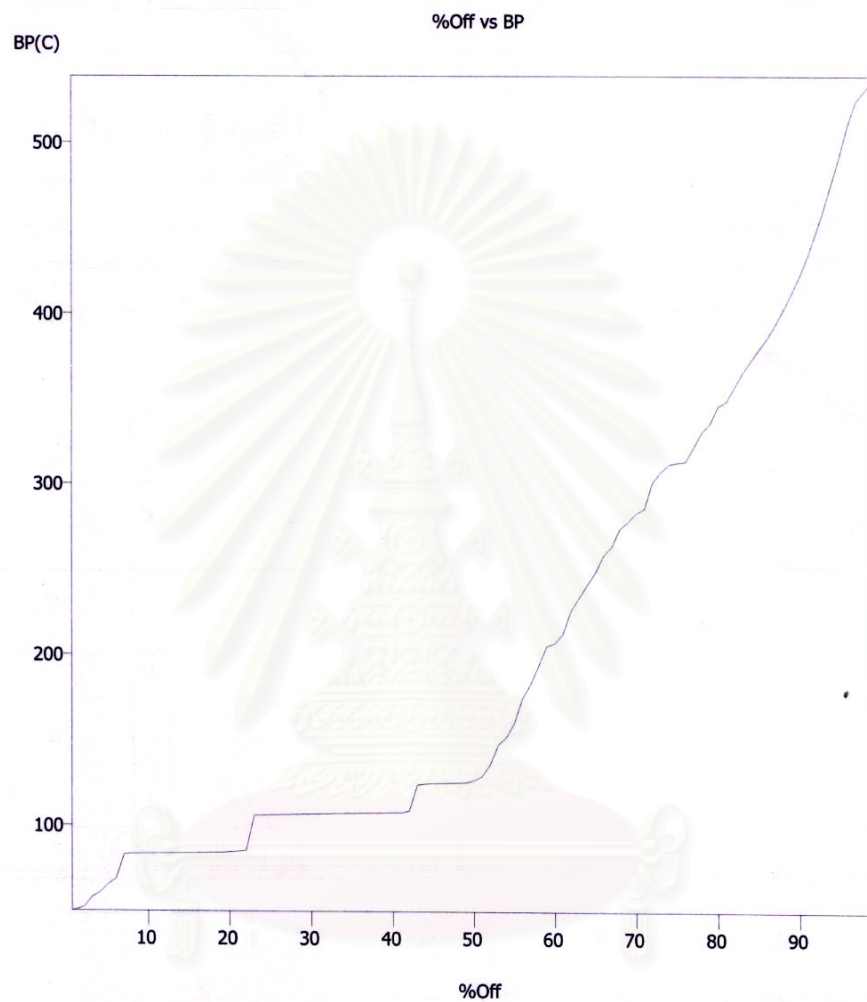
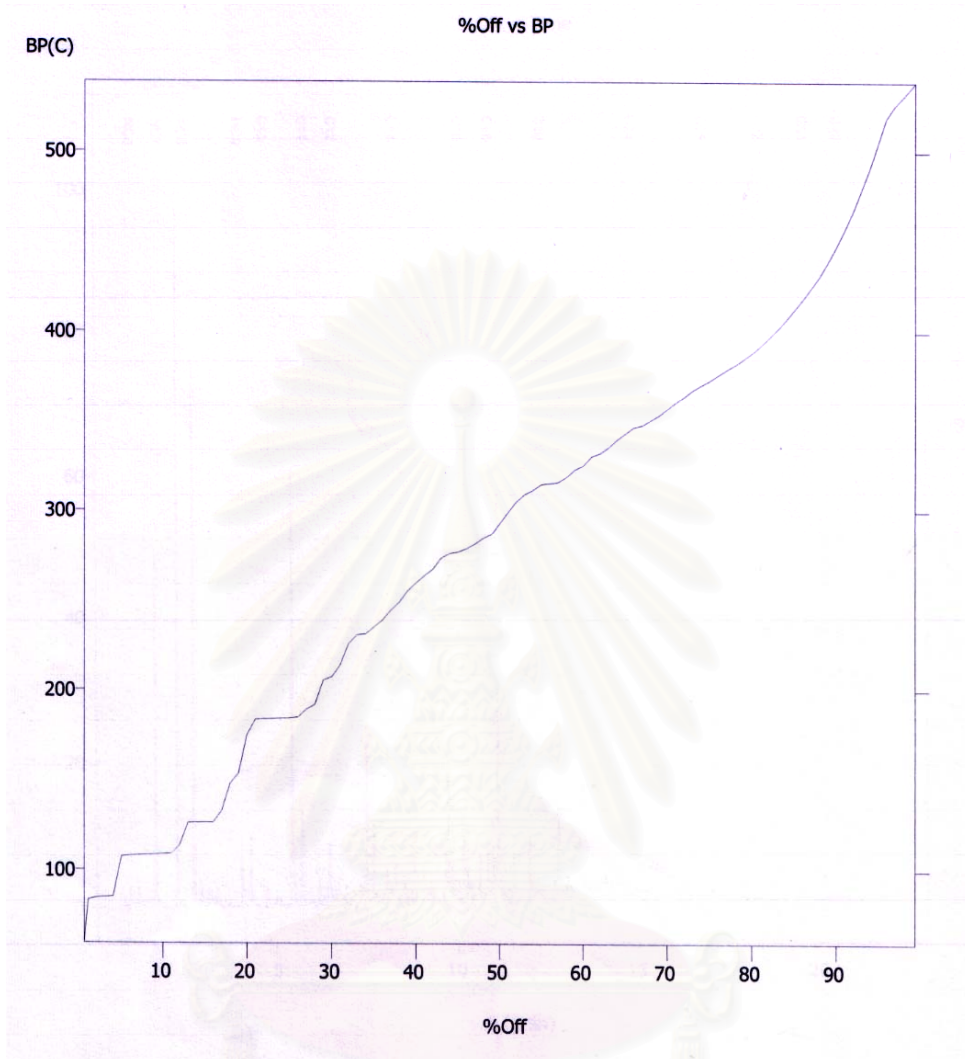


Figure B.8 Oil composition at condition 90 min of reaction time, 430 °C of reaction temperature, 1.25% of HZSM-5 catalyst, 200 psig of hydrogen and by GC Simulated Distillation.



สถาบันวิทยบริการ
จุฬาลงกรณ์มหาวิทยาลัย

Figure B.9 Oil composition at condition 100 psig of hydrogen, 430 °C of reaction temperature, 1.25% of HZSM-5 catalyst and 60 min of reaction time by GC Simulated Distillation.



สถาบันวิทยบริการ
จุฬาลงกรณ์มหาวิทยาลัย

Figure B.10 Oil composition at condition 300 psig of hydrogen, 430 °C of reaction temperature, 1.25% of HZSM-5 catalyst and 60 min of reaction time by GC Simulated Distillation.

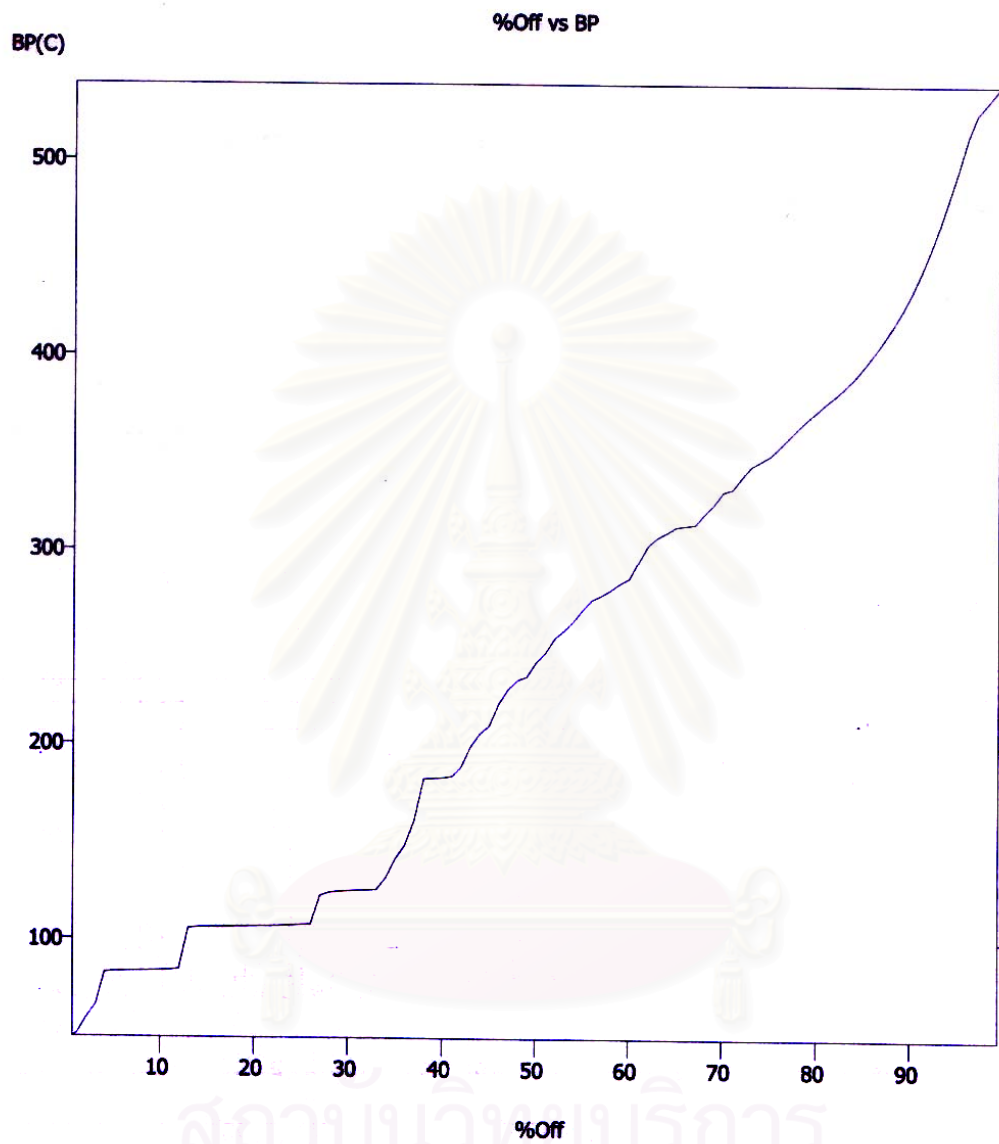


Figure B.11 Oil composition at condition 200 psig of hydrogen, 430 °C of reaction temperature, non-catalyst and 60 min of reaction time by GC Simulated Distillation.

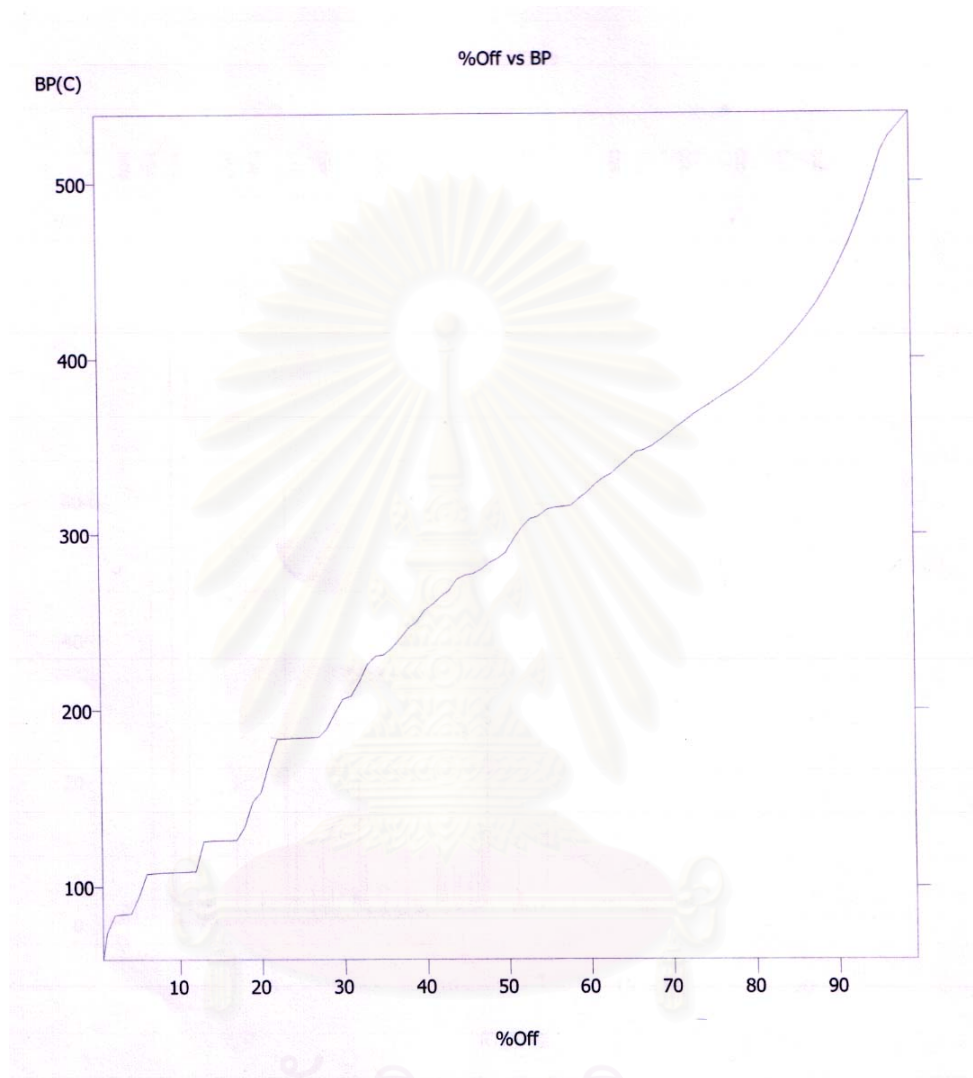


Figure B.12 Oil composition at condition 430 °C of reaction temperature, 1.25% of HZSM-5 catalyst, non-hydrogen and 60 min of reaction time by GC Simulated Distillation

VITA

Mrs.Rattana Boonprasert was born in Saraburi, Thailand on July 1, 1972. She received her Bachelor Degree of Education (B. Ed.) Major subject: Science-Chemistry from Srinakharinwirot University in 1995. She continued her Master's study at Petrochemical and Polymer Science Department, Graduate School, Chulalongkorn University in 2002 and completed the program in 2004.



สถาบันวิทยบริการ
จุฬาลงกรณ์มหาวิทยาลัย